



Identification of a novel hatching factor for potato cyst nematode and investigation of its biosynthesis

清水, 宏祐

(Degree)

博士 (農学)

(Date of Degree)

2022-03-25

(Date of Publication)

2024-03-25

(Resource Type)

doctoral thesis

(Report Number)

甲第8370号

(URL)

<https://hdl.handle.net/20.500.14094/D1008370>

※ 当コンテンツは神戸大学の学術成果です。無断複製・不正使用等を禁じます。著作権法で認められている範囲内で、適切にご利用ください。



Doctoral Dissertation

**Identification of a novel hatching factor for
potato cyst nematode and investigation of its
biosynthesis**

ジャガイモシストセンチュウに対する新規ふ化促進物質の
同定とその生合成の解析

January, 2022

Kosuke SHIMIZU

Graduate school of Agricultural Science

Kobe University

Contents	
<u>General introduction</u>	<u>1-6</u>
<u>Chapter 1</u>	<u>7-21</u>
Hatching stimulation activity of steroidal glycoalkaloids toward the potato cyst nematode, <i>Globodera rostochiensis</i>	
Introduction	7
Materials and methods	8-10
Results and discussion	11-14
Concluding remark	14-15
Figures and tables	16-21
<u>Chapter 2</u>	<u>22-55</u>
Isolation and structure determination of a novel hatching factor, solanoecelepin B, from potato hydroponic culture solution	
Introduction	22
Materials and methods	22-28
Results	28-33
Discussion	34-35
Figures and tables	36-55
<u>Chapter 3</u>	<u>56-87</u>
Identification of the oxygenase genes involved in solanoecelepin B biosynthesis from tomato	
Introduction	56
Materials and methods	57-61
Results	61-65
Discussion	65-67
Figures and tables	68-87
<u>Concluding discussion</u>	<u>88-89</u>
<u>Acknowledgement</u>	<u>90</u>
<u>References</u>	<u>91-97</u>

General introduction

Plants produce a vast array of organic compounds, called plant specialized metabolites (PSMs)¹. In general, PSMs are not directly involved in essential processes such as plant growth and development, but PSMs possess various biological activities and are thought to have been acquired evolutionarily by each plant species to use as defense compounds against pathogens or herbivores and for environmental adaptation. Therefore, PSMs are thought to have important roles in the interaction between plants and other organisms. Since plants have to co-exist with numerous microorganisms in soil, they excrete organic compounds including PSMs from the roots to build and control their beneficial environment called rhizosphere^{2,3}. For example, isoflavones predominantly in legume plants which are excreted from roots are utilized as signal molecules to establish symbiotic interactions with Rhizobia, resulting in effective gain of nitrogen nutrition⁴. On the other hand, PSMs excretion causes a negative effect on plant themselves. Some plant parasitic nematodes utilize the secreted PSMs to recognize the presence of host plants.

Plant parasitic nematodes are one of the most harmful pests, and their damage to the crop production is estimated at \$US80 billion per year^{5,6}. Among them, cyst nematodes are one of the most economically important pests. Cyst nematodes are the group of highly evolved sedentary endoparasites consisting of the genera of *Globodera* and *Heterodera* and cause serious losses in important crop production in over 50 countries^{5,6,7}. Unlike other plant parasitic nematodes, such as root-knot nematodes, the host range of cyst nematodes is narrow and strictly host-specific⁸. For example, soybean cyst nematodes (SCNs), *Heterodera glycines* Ichinohe, parasitize only a few species among the Fabaceae family, such as soybean (*Glycine max*), azuki bean (*Vigna angularis*), and common bean (*Phaseolus vulgaris*), and potato cyst nematodes (PCNs) specifically

parasitize a few species among the *Solanaceae* family, such as potato (*Solanum tuberosum*) and tomato (*Solanum lycopersicum*). Two PCN species, *Globodera rostochiensis* and *G. pallida*, have been reported in Japan. The life cycle of cyst nematodes is highly synchronized to that of the host plants⁶. The dormant eggs are covered with a cyst, which is the dead body of female nematode, and are able to remain dormant for 20 years until the arrival of host plants. The hatching of the cyst nematode eggs occurs in response to the host-derived compounds called hatching factors (HFs) excreted from roots, and then the second-stage juveniles (J2) migrate and invade the host plant roots. HFs are thought to be the compounds which are actively biosynthesized and excreted by host plants, but HFs are successfully and efficiently used by cyst nematodes as signal molecules to recognize the presence of a preferred host plant around them. This hatching behavior depending on HFs is a key feature to determine the high host specificity of cyst nematodes by detecting the presence of host plants near the cyst nematode eggs (Figure I).

To date, three HFs for SCN, namely glycinoclepin A (GEA), glycinoclepin B (GEB), and glycinoclepin C (GEC), have been isolated from the extracts of the roots of kidney bean (*Phaseolus vulgaris*)^{9,10} (Figure II). In addition, solanoclepin A (SEA) which shows the hatching stimulation (HS) activity at the concentration ranging from 1×10^{-8} to 1×10^{-10} g ml⁻¹, has been isolated from the root leachates of potatoes and tomatoes and identified as a HF for PCN eggs (Figure II)^{11,12,13}. In terms of their chemical structures, all the four HFs are classified as triterpenoids. Due to the lack of development of analytical methods to detect HFs, however, little is known about their biosynthesis, secretion mechanism, and function in plants themselves. Moreover, although the total organic synthesis of GEA^{14,15,16,17,18} and SEA¹³ has been developed, it is difficult to

develop the synthetic analogs of HFs because of their structural complexities. Therefore, the HF-mediated hatching mechanism of cyst nematode eggs is also still largely unknown.

In addition to SEA, it has been reported that several kinds of natural compounds, such as α -solanine and α -chaconine, show weak but significant HS activity toward PCNs eggs^{19,20} (Figure II). Both α -solanine and α -chaconine are well known steroidal glycoalkaloids (SGAs), a member of triterpenoids, that are specifically present in Solanaceae plants, and abundant amounts of SGAs are accumulated in potato particular tissues including roots. Therefore, it might be possible that SGAs play a role as HFs toward PCNs in nature.

This study aimed to elucidate major HFs showing the actual HS activity in host plant root exudates and to identify their biosynthetic genes in the host plants. In “Chapter 1”, I evaluated the contribution of SGAs on HS activity of tomato and potato hairy roots culture solution. SGAs, such as α -solanine, α -chaconine, and α -tomatine, showed significant HS activity, despite being remarkably less activities than that of SEA. The estimated SGAs levels in the hairy root culture solution were low and nonconcordant with the HS activity detected in the culture solution, suggesting that the HS activity of SGAs contributed little. I also conducted the analysis of structure-activity relationship. The results revealed that the structural requirements of the HS activity of SGAs are dependent on the sugar moieties attached at the C3-hydroxy group and the alkaloid property of their aglycones. The stereochemistry in the EF rings of their aglycones also affected the strength of the HS activity. In “Chapter 2”, we identify a novel HF from potato hydroponic culture solution. HFs in potato hydroponic culture solution were collected using synthetic absorbents, and after several purification steps including liquid phase extraction, open column chromatography, and preparative HPLC, a novel HF was detected in addition to

previously known SEA. The novel HF was isolated, and its chemical structure was determined as solanoeclepin B (SEB). In the culture solution of tomato hairy roots, SEB was detected by using LC-MS/MS analysis, but SEA was not, suggesting that SEB is a major HF secreted from tomato hairy roots. In “Chapter 3”, we searched for the genes involved in solanoeclepin biosynthesis. Biochemical studies suggested that HF biosynthesis is specifically occurred in roots and that oxygenases such as cytochrome P450 monooxygenase (CYP) and 2-oxoglutarate dependent dioxygenase (DOX) are involved in HF biosynthesis. The genes encoding CYP or DOX, which are specifically expressed in roots, were selected as candidate biosynthetic genes, and the disruption of the candidate genes with CRISPR/Cas9 system was conducted to evaluate their contribution to the HS activity in the hairy roots culture solution. As a result, three *DOX* genes, *SIDOX60*, *SIDOX70*, and *SIDOX80*, and two *CYP* genes, *SICYP749A19*, *SICYP749A20*, were identified as the genes involved in SEB biosynthesis. Based on these results, the application on the development of counter measure against PCN was described in “Concluding discussion”.

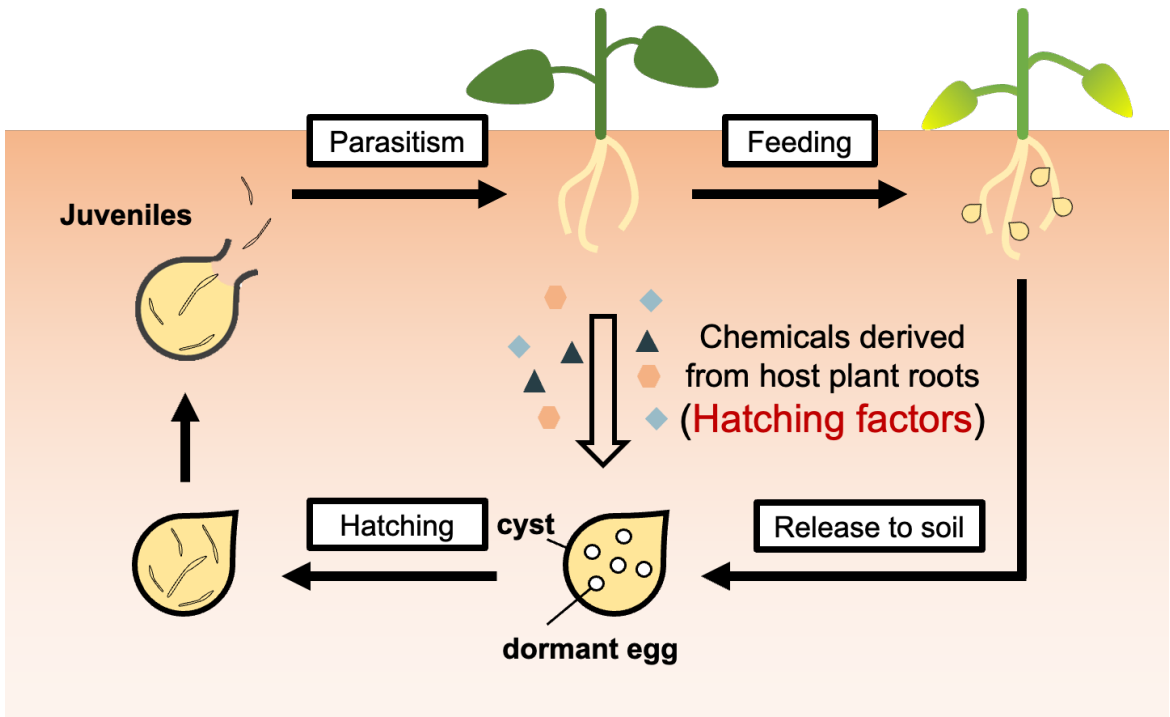


Figure I. The life cycle of cyst nematodes.

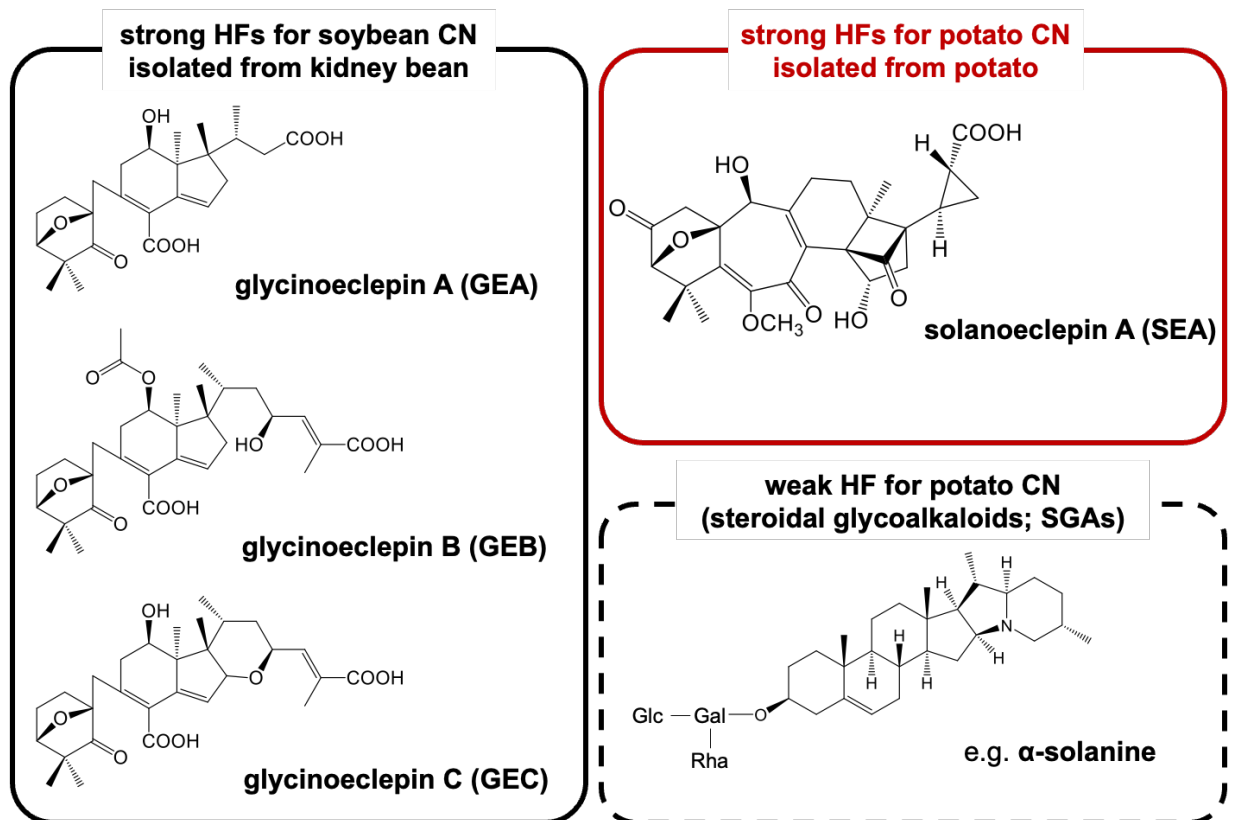


Figure II. The structures of hatching factors (HFs) for potato cyst nematodes (PCNs) and soybean cyst nematodes (SCNs).

Chapter 1

Hatching stimulation activity of steroidal glycoalkaloids toward the potato cyst nematode, *Globodera rostochiensis*.

Introduction

As described in “General introduction”, solanoelepin A (SEA) is an only hatching factor (HF) identified as the compounds possess high HS activity toward the potato cyst nematode (PCN) eggs, whereas the steroidal glycoalkaloids (SGAs) possess weak HS activity (Figure 1-1). Since the SGAs are the abundant compounds in potato and tomato, it is possible that SGAs show and contribute the HS activity toward PCN eggs in nature.

PCNs are the harmful pest and cause serious damage on crop production such as potato, and tomato. The characteristic hatching mechanism of PCNs could be a good target to establish the effective counter measures against PCNs. To achieve this, the detailed understanding of the hatching mechanism is required, however, little is known about the HF-mediated hatching mechanism. It is difficult to reveal the structure-activity relationship of the HS activity due to the structural complexity. In contrast, SGAs are well-known plant specialized metabolites (PSMs) and there are structurally diverse SGAs in nature.

In this study, I analyzed the HS activity of culture medias of hairy roots of potato and tomato toward *G. rostochiensis* eggs. I determined the SGA concentrations in the culture medias, and evaluated the contribution of SGAs (α -solanine, α -chaconine, and α -tomatine) to the detected HS activity. I also investigated the HS activities of other related triterpene compounds and estimated whether SEA and SGAs stimulate the hatching of PCN eggs in a similar manner.

Materials and methods

Chemicals

Synthetic solanoelepin A (SEA) was provided by Prof. Keiji Tanino (Hokkaido University). The authentic samples of α -solanine, α -chaconine, solanidine, solasonine, dioscin, and diosgenin were purchased from Sigma-Aldrich Japan (Tokyo, Japan). α -Tomatine and tomatidine were purchased from Tokyo Chemical Industry Co., Ltd. (Tokyo, Japan) and ChromaDex (Irvine, CA, USA), respectively. The contaminants in α -tomatine and tomatidine were removed using high-performance liquid chromatography (HPLC). α -Solamarine and β -solamarine were purified from diploid potato clone 97H32-6 in our laboratory and identified with liquid chromatography–mass spectrometry (LC-MS) and nuclear magnetic resonance (NMR) analyses.

Plant materials and generation of hairy roots

The tomato plant used in this chapter was *S. lycopersicum* cv Micro-Tom (TOMJPF00001), obtained from the National BioResource Program (NBRP) (MEXT, Japan). The surface-sterilized seeds of tomato were germinated and cultivated under the condition of 25°C with 16/8-h light/dark photoperiod on Murashige and Skoog (MS) medium containing 1.5% (w/v) sucrose and 0.3% (w/v) Gelrite (Wako). The potato plant used in this chapter was *S. tuberosum* cv Sassy. The Sassy *in vitro*-grown shoots were grown at a temperature of 20°C with 16/8-h light/dark on MS medium containing 2% (w/v) sucrose and 0.3% (w/v) Gelrite. The common bean plant used in this chapter was *Phaseolus vulgaris* cv Honkintoki purchased from Takii & Co. (Kyoto, Japan). The common bean seeds were germinated and cultivated in a way similar to that of the tomato described above. The hairy roots of tomato and potato were obtained by inoculation of

the stems with *Agrobacterium rhizogenes* strain ATCC15834 as described by Thagun et al. (2016)²¹. The generation of common bean hairy root was conducted in the same manner as that of the tomato and potato plants, with minor alterations as follows: the 5-day-old seedlings were infected by *A. rhizogenes* strain K599. The infected seedlings and hairy roots that emerged from the infected sites were subcultured every two weeks on a medium containing MS salts, B5 vitamins, 500 µg ml⁻¹ carbenicillin, 2% (w/v) sucrose, and 0.3% (w/v) Gelrite.

SGAs analysis

The hairy roots of tomato and potato were cultured for 14 days with 50 ml of liquid B5 medium containing 2% (w/v) sucrose and 250 µg ml⁻¹ cefotaxime in 200-ml glass flasks. The hairy root culture media were used for SGA analysis and hatching assays. The SGAs secreted from the hairy roots were extracted from the 500 µl culture media with equal volume of *n*-butanol three times. The extracts were evaporated, dissolved in methanol, and analyzed by LC-MS analysis as previously described²². Selected ion monitoring (SIM) modes with *m/z* 578.6, 868.9, and 852.8 were used to detect α-tomatine, α-solanine, and α-chaconine respectively.

Hatching assays

The common bean hairy roots were suspended for 2 weeks with 50 ml of liquid medium containing MS salts, B5 vitamins, 2% (w/v) sucrose, and 250 µg ml⁻¹ cefotaxime in 200-ml glass flasks. Then, 1 ml of culture media was collected and frozen at -30°C. The hatching stimulation activities of the hairy root media and each SGA compound toward *Globodera rostochiensis* eggs were investigated. *G. rostochiensis* pathotype Ro1, a

population originally isolated from a field in Kucchan-cho, Hokkaido, Japan, was propagated on greenhouse-grown potato cultivar Irish Cobbler. After the potato had died, the soil containing the cysts was lightly dried and stored at 4°C for 6 months at least in order to break dormancy. The cysts were isolated from the soil by the dry flotation method, picked out from the isolate under a binocular, and incubated in distilled water for 2 weeks at 18°C. Subsequently, an egg suspension was prepared by crushing the cysts and removing broken pieces of cysts, dead eggs, and hatched juveniles as completely as possible. After the egg density of the suspension was adjusted to approximately 600 eggs per milliliter, Tween 20 (polyoxyethylene [20] sorbitan monolaurate) was added to the egg suspension with 0.05% concentration to prevent nematode eggs aggregation. Then, 1 ml of the egg suspension were added to each glass vials (volume; 13.5 ml, inside diameter; 21 mm, height; 50 mm) and 1 ml of each sample was added with double concentration of the test conditions; SGAs: 1 and 5 µM, tomato hairy root culture medium: 1 : 1000, 1 : 5000, and 1 : 25000 dilution, potato hairy root culture medium: 1 : 100, 1 : 500, and 1 : 2500 dilution, common bean hairy root culture medium: 1 : 250 and 1 : 1000 dilution. The glass vials were added 1 ml of distilled water or 1 : 20 diluted B5 medium containing 250 µg ml⁻¹ cefotaxime were prepared as negative controls. I also prepared the glass vials containing SEA with the concentrations of 1 and 100 pg ml⁻¹ as positive controls. Each vial was incubated at 18°C for approximately 2 weeks. Subsequently, 1 ml of each vial was taken out and transferred to Syracuse dishes, and the hatched juveniles and unhatched eggs were counted under a binocular. Although each assay was conducted in duplicate, the negative control assay was conducted in triplicate.

Result and discussion

HS activity of potato and tomato hairy root culture media

Because of their fast and bacteria-free growth, I used the hairy roots as plant materials. I first estimated the HS activity of the potato and tomato hairy root culture media toward PCN (*Gr*) eggs. Deionized water almost did not induce a hatching response of the PCN eggs, whereas the PCN eggs hatched in response to SEA at a quite low concentration (100 pg ml^{-1}). The tomato and potato hairy root culture media showed HS activity for PCN eggs, whereas the culture media without hairy roots did not show any HS activity (Figure 1-2A, B). The tomato hairy root culture media showed HS activity that was ten times higher compared with that of the potato hairy root culture media. The solution of tomato culture media that was diluted 1,000 times with water exhibited a HS activity equivalent to 100 pg ml^{-1} of SEA, suggesting that the tomato hairy root culture media contained HFs that possess a HS activity comparable to SEA. The common bean hairy root culture media showed no significant HS activity for PCN eggs (Figure 1-2C), indicating that the HFs for PCN eggs are not secreted from the hairy roots of a non-host plant, such as the common bean.

As previously reported²³, I showed that bacteria-free culture media of the host plant hairy roots can strongly induce the hatching of the PCN eggs, indicating that the HFs are definitely biosynthesized and secreted by the hairy roots. Hairy roots are well used materials in the field of plant secondary metabolism because of its stable production of metabolites. Moreover, gene disruption using genome editing tools, such as CRISPR/Cas9, has been successfully established²⁴. Therefore, hairy roots are suitable materials to reveal the biological and physiological biosynthesis and secretion of HFs.

HS activity of α -tomatine, α -solanine and α -chaconine

I then analyzed the HS activities of steroidal glycoalkaloids (SGAs), which are one of the most abundant secondary metabolites specifically biosynthesized in *Solanaceae* plants. The hatching assays were performed at 1 or 5 μM of SGAs in water because the organic solvent inhibits the hatching of the PCN eggs. As previously reported²⁰, α -solanine and α -chaconine at 1 or 5 μM exhibited significant HS activities, and α -tomatine also showed HS activity at 5 μM . The hatching rate treated with 5 μM of α -chaconine was $48.6 \pm 1.1\%$, while SEA at 100 pg ml^{-1} (about 2 pM) induced the hatching of PCN eggs over 90% (Figure 1-2, 1-3), indicating that the HS activities of SGAs are quite weaker compared with that of SEA.

In order to evaluate the contribution of SGAs to the HS activities detected in the hairy root culture media, I estimated the SGA levels in culture media of tomato and potato hairy roots by LC-MS analysis (Figure 1-4). α -Tomatine was detected in the tomato hairy root culture media, and its concentration was estimated to be $2.90 \pm 0.36 \mu\text{M}$. Similarly, α -solanine and α -chaconine were detected in the potato hairy root culture media, and those concentrations were estimated to be $0.14 \pm 0.0061 \mu\text{M}$ and $0.071 \pm 0.0033 \mu\text{M}$, respectively. The 1 : 1000 diluted solution of the tomato culture media contained less than 1 nM α -tomatine, whereas the hatching rate of the diluted solution was about 90%, indicating that α -tomatine almost do not affect the HS activity detected in the tomato hairy root culture media. Similarly, α -solanine and α -chaconine are of little contribution to the HS activities detected in the potato hairy root culture media. In field-grown plants, the secretion of SGAs could be higher than that in the hairy root culture, and the concentration of SGAs accumulated in the rhizosphere might be affected by their stability and microbial degradation in soils. SGA-modified and/or

SGA-deficient plants by gene disruption of SGA biosynthetic genes, which were previously identified and characterized in tomato and potato^{24,25,26,27,28,29} can be examined to clarify the contribution of SGAs in the fields for future experiments.

Structure–activity relationship of SGAs for HS activity

Next, I analyzed the HS activities of several steroidal compounds, such as SGAs, steroidal saponins, and their aglycones (Figure 1-5). Tomatidine, the aglycone of α -tomatine, did not induce the hatching of PCN eggs at 1 and 5 μ M, and solanidine, that of α -solanine and α -chaconine, also showed little HS activity. These results suggested that the sugar moieties attached at the C3-hydroxyl group of the aglycones are required for the HS activity by SGAs (Figure 1-6A). Moreover, α -solamarine, β -solamarine, and solasonine, which are the members of SGAs that accumulated in the *Solanum* species, possessed significant HS activities, and solasonine showed the strongest HS activity among all the tested SGAs (Figure 1-6B). The hatching rates of α -chaconine and β -solamarine were higher than that of α -solanine or α -solamarine, respectively, suggesting that chacotriose is more active than solatriose as the sugar moieties attached at the C3-hydroxyl group of the aglycones (Figure 1-6B). In contrast, dioscin and its aglycone diosgenin did not show significant HS activity (Figure 1-6A). The sugar moiety of dioscin is chacotriose, which is identical to those of α -chaconine and β -solamarine, but the aglycone of dioscin does not contain nitrogen. Therefore, these results suggested that the HS activity of SGAs depend not only on the presence of the sugar moieties but also on the alkaloid property of the aglycone. The HS activity of solasonine was more than 5 times stronger than that of α -solamarine; while these two SGAs share the same sugar moieties, namely solatriose (Figure 1-6B). The aglycones of solasonine and α -

solamarine are (22*R*, 25*R*)-spirosolane and (22*S*, 25*S*)-spirosolane, respectively, suggesting that the stereochemistry in the EF rings also affects the strength of the HS activity of SGA.

Both of SEA and SGAs are classified as triterpenoids; however, their structures are quite different. SEA is a unique and highly oxygenated triterpenoid consisting of heptacyclic skeleton with three- to seven-membered carbocycles. The 6,6-dimethyl-7-oxabicyclo[2.2.1]heptan-2-one in the A-ring is one of the characteristics of SEA. On the other hands, SGAs have the sugar moieties attached to C3-hydroxyl group in the A-ring, and the aglycone is a canonical steroidal skeleton with a single nitrogen. Our results of the hatching assays using SGAs suggested that the prerequisite of the sugar moieties and nitrogen in the EF ring for the HS activity, whereas SEA does not have a sugar moiety or nitrogen. This inconsistency might be due to the occurrence of different recognition mechanisms for SGAs and SEA by the PCN eggs.

Concluding Remark

Unlike other plant parasitic nematodes, cyst nematodes also establish strict host specificity in terms of the hatching mechanism of their eggs. This feature considerably enables efficient proliferation and alternation of generations. Plants produce diverse kinds of specialized metabolites which have ecological functions in plant-microbe communication in rhizosphere^{30,31}. Therefore, they could be suitable indicators of the presence of host plants near the dormant eggs of cyst nematodes. The hatching response of PCN eggs for a broad range of triterpenoid compounds suggested that there might have been co-evolution between triterpenoid biosynthesis in host plants and the recognition mechanism in cyst nematodes, and that cyst nematodes might evolutionally

select SEA as a specific HF. Our findings are helpful for further research focusing on the biosynthesis and secretion mechanism of hatching factors, and hairy roots are suitable materials for these studies.

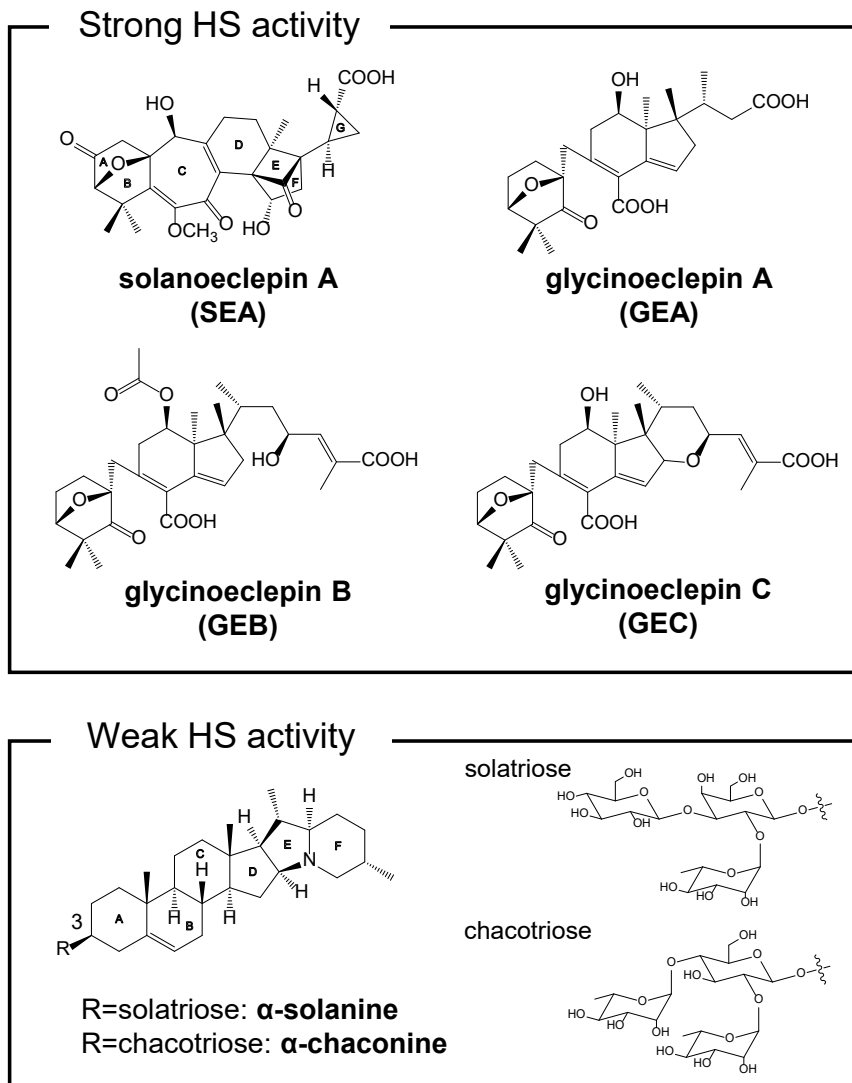


Figure 1-1. Hatching factors (HFs) of cyst nematode eggs.

The upper group includes HFs which were isolated using hatching stimulation (HS) activity as an indicator. The lower group includes HFs reported to show weak but significant HS activity.

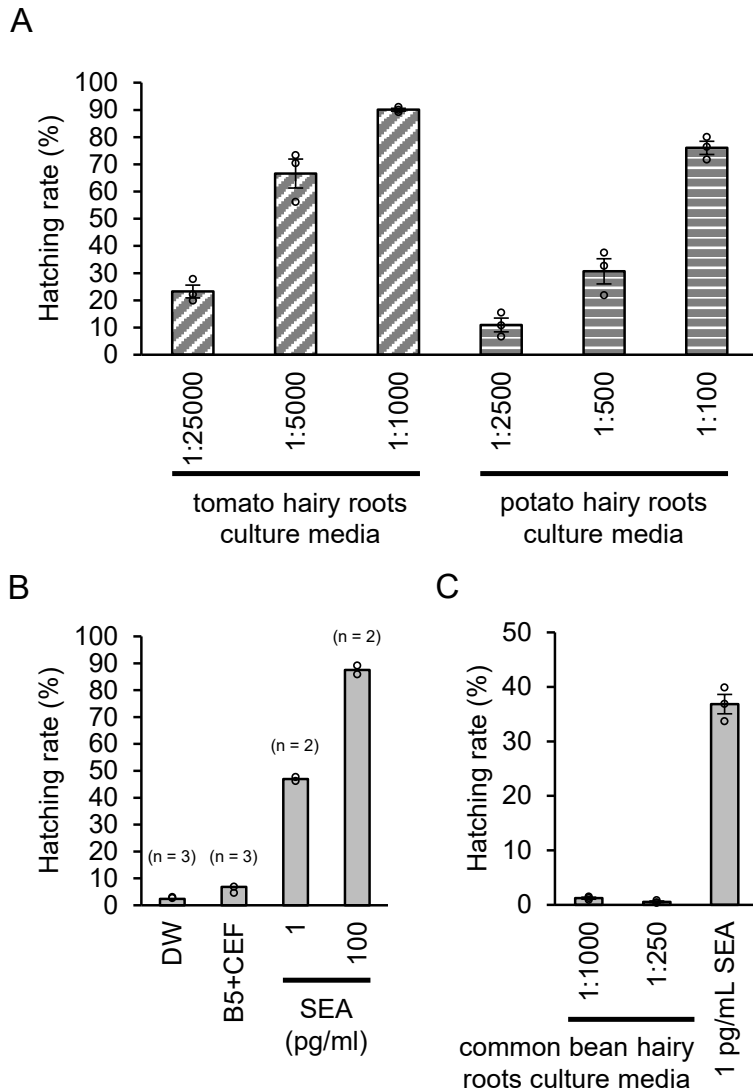


Figure 1-2. HS activity of the hairy root culture media.

The hatching rates (%) of PCN eggs incubated in culture media (A) with host hairy roots, (B) without hairy roots, and (C) with non-host hairy roots are shown. (A) The values are presented as mean \pm SE. The samples were harvested from three independent flasks, and three series of dilution are shown for the culture media. The hatching assay was conducted in duplicate. (B) The values are presented as mean \pm SE. The hatching assay was conducted in triplicate for distilled water (DW) and 1:20 diluted B5 medium containing 250 $\mu\text{g ml}^{-1}$ cefotaxime (B5+CEF), and in duplicate for each concentration of SEA. (C) The hatching assay was conducted in triplicate. Two series of dilutions are shown for the common bean hairy root culture media.

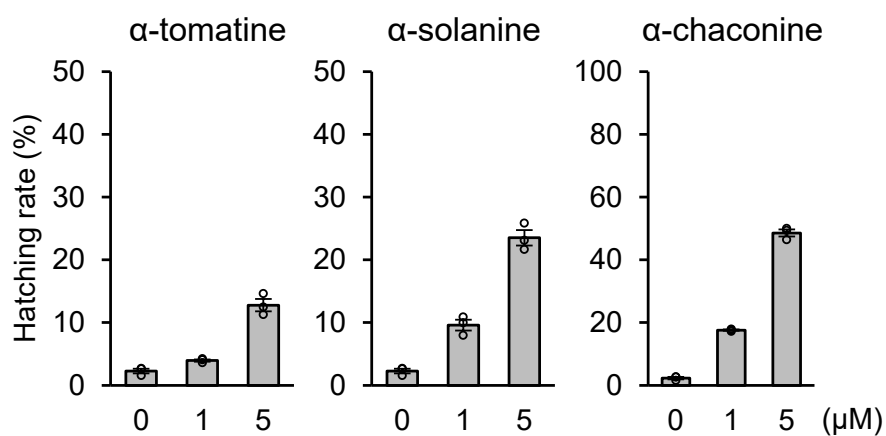


Figure 1-3. HS activity of steroidal glycoalkaloids (SGAs).

The hatching rates (%) of PCN eggs incubated with 0, 1, and 5 μM of α-tomatine, α-solanine, and α-chaconine, respectively, are shown. The values are presented as mean ± SE in triplicate.

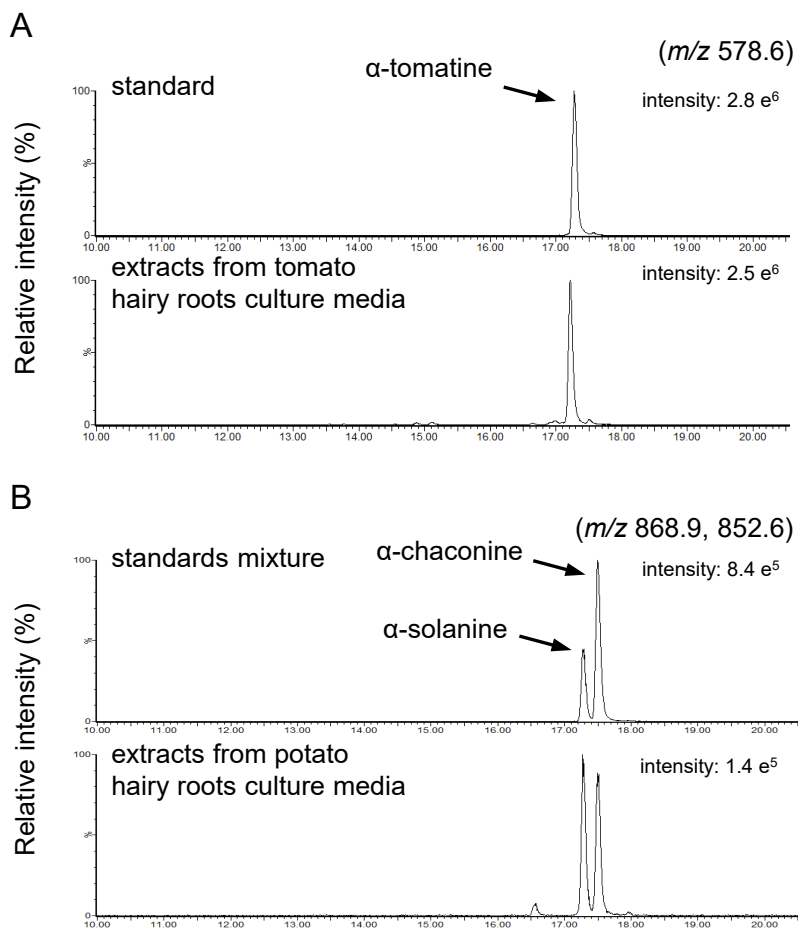
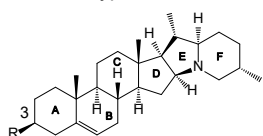


Figure 1-4. The analysis culture media of (A) tomato and (B) potato hairy roots. The selected ion monitoring (SIM) chromatograms obtained by LC-MS analysis are shown.

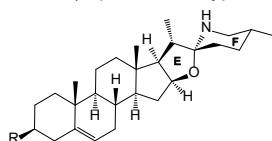
Steroidal glycoalkaloids (SGAs)

solanidane type



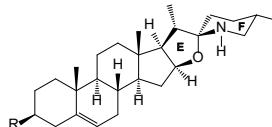
R=1: **solanidine**
R=2: **α -solanine**
R=3: **α -chaconine**

(22*R*,25*R*)-spirosolane type

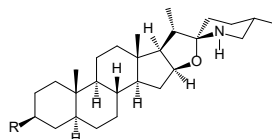


R=1: **solasodine***
R=2: **solasonine**

(22*S*,25*S*)-spirosolane type



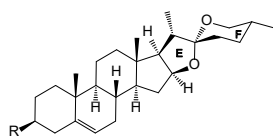
R=1: **dehydrotomatine***
R=2: **α -solamarine**
R=3: **β -solamarine**
R=4: **dehydrotomatine***



R=1: **tomatidine**
R=4: **α -tomatine**

Steroidal saponin

spirostane type



R=1: **diosgenin**
R=3: **dioscin**

R1: -OH

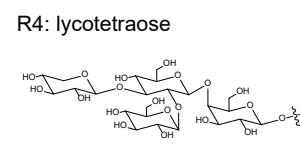
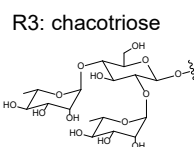
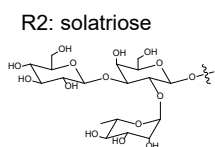


Figure 1-5. Several kinds of triterpenoid compound are shown.

Asterisk shows the compound that was not tested in this study.

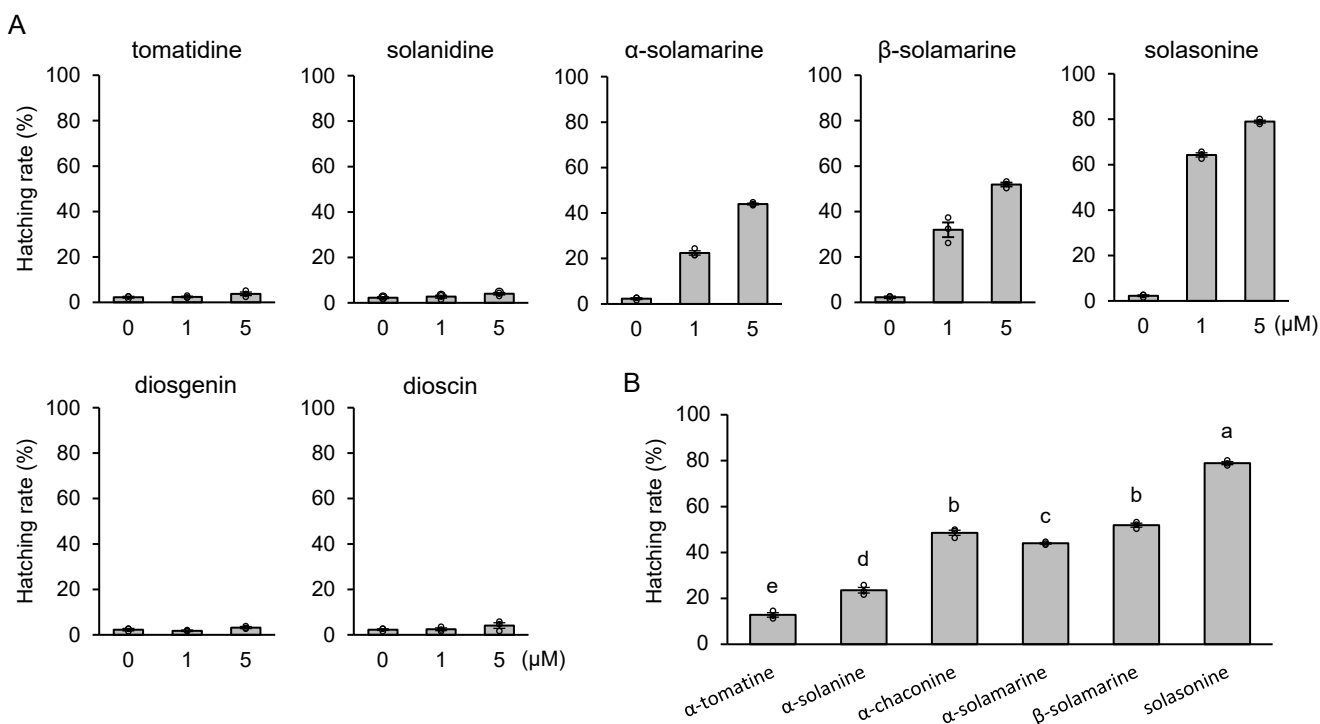


Figure 1-6. HS activity of several kinds of triterpene compound.

(A) The hatching rates (%) of PCN eggs incubated with 0, 1, and 5 μM of SGAs; steroidal saponins, and their aglycone. The values are presented as mean \pm SE in triplicate. (B) The hatching rates (%) of PCN eggs incubated with 5 μM SGAs, which were confirmed to exhibit HS activity. The values are presented as mean \pm SE in triplicate. The different letters indicate statistical differences by Tukey's test ($p < 0.05$).

Chapter 2

Isolation and structure determination of a novel hatching factor, solanoeclepin B, from potato hydroponic culture solution.

Introduction

As described in “General introduction”, solanoeclepin A (SEA) is the only natural compound that has been identified as a hatching factor (HF) toward potato cyst nematode (PCN) eggs, and its HS activity was also confirmed by synthetic SEA. However, the presence of SEA in hydroponic culture solution of potato and tomato has not been confirmed using by the analytical method to date. Similarly, although the hairy roots culture solutions of potato and tomato showed high HS activity as described in “Chapter 1”, SEA was not detected in them using LC-MS/MS analysis. These results suggested the presence of an unidentified compound, differed from SEA, that functions as a major HF in tomato and potato.

In this chapter, purification of HFs from potato hydroponic culture solution was conducted. Whereas SEA was detected in the purified fraction, a novel HF was identified from another purified fraction. Structural analysis indicated that the molecular mass of the novel HF is two mass larger than that of SEA, due to the substitution at the C-2 ketone group of SEA to a hydroxy group. Therefore, I have determined its chemical structure and designated it as solanoeclepin B (SEB).

Materials and methods

Chemicals

Synthetic solanoeclepin A (SEA) was provided by Prof. Keiji Tanino (Hokkaido

University).

Hatching assay-based purification of hatching factors from potato hydroponic culture solution

Total of approximately 30 L of Sepabeads SP207 resin (Mitsubishi Chemical Corp.) placed in potato hydroponic culture system from June to October 2018 in Hokkaido Agricultural Research Center, National Agriculture and Food Research Organization (HARC/NARO), where the amount of hydroponic solution was estimated to be approximately 80,000 L per year and the resin was replaced every month, was provided by Dr. Atsuhiko Kushida (HARC/NARO). Fifteen liters of resin was transferred into flask and eluted twice with three times resin volumes of methanol by shaking for 1 hour at room temperature. The methanol eluents were dried *in vacuo* and re-dissolved in 500 ml of methanol to remove methanol insoluble materials. The methanol soluble fraction (20.9 g) was dried *in vacuo*, dissolved in 1 L of water, and treated three times with the same volume of *n*-hexane. The remaining aqueous phase was adjusted pH 3 with 1 N HCl and extracted three times with 1 L of ethyl acetate. The acidic ethyl acetate phase (4.8 g) was dried *in vacuo*, dissolved in 5% (v/v) aqueous methanol, and loaded onto five independent Sep-Pak C₁₈ cartridge (Vac 35 cm³, 10g; Waters) pre-washed and equilibrated with five column volumes of methanol and 5% (v/v) aqueous methanol, respectively. Each cartridge was washed with five column volumes of 5% (v/v) aqueous methanol and eluted with five column volumes of 20% (v/v) aqueous methanol and methanol. Because of the more potent HS activity, the methanol fraction was conducted to the subsequent purification processes. The methanol fraction (3.4 g) was dried *in vacuo*, re-dissolved in 30 mL of methanol, and passed through a strong cation exchanger

Dowex 50 (H⁺ form, 200 ml; Sigma-Aldrich) with 1 L of methanol. The non-cationic pass-through fraction (2.8 g) was dried *in vacuo*, re-dissolved in 7 ml of methanol, and subjected to a Sephadex LH-20 column chromatography (150 ml; GE Healthcare). In Sephadex LH-20 column chromatography, elution was conducted with 445 ml of methanol, where fractionation was as follows: fraction 1: 45 ml, fraction 2: 20 ml, fraction 3-21: 5 ml each, fraction 22: 65 ml, fraction 23: 175 ml. The active fractions of fraction 11-16 and 17-20 were separated as Frs-fast and Frs-late, respectively, and the subsequent purification process was conducted independently. Frs-fast (1,664 mg) and Frs-late (687 mg) were dried *in vacuo*, re-dissolved in 10 mL of methanol, and loaded onto a strong anion exchanger Dowex 1 (acetate form, 400 mL, Sigma-Aldrich). After the column was washed with 2 L of methanol, elution was conducted three times with 650 ml of methanol containing 0.1 or 1 N acetic acid. In terms of the relative activity by fraction weight, the fraction 2 and 3 of methanol containing 1 N acetic acid derived from Frs-late was subjected to following HPLC preparation. The active fraction was dissolved in 100 µl of 5% (v/v) aqueous acetonitrile and subjected to a reversed phase HPLC connected to an Atlantis T3 column (10 × 150 mm, 5 µm; Waters) protected by an Atlantis T3 Prep Guard Cartridge (10 × 10 mm, 5 µm; Waters). The mobile phase consists of solvent A (0.1% formic acid in water) and solvent B (0.1% formic acid in acetonitrile) with the flow rate at 5.0 ml min⁻¹ using linear gradient system as follows; 5% B at 0 min and hold 5 min, ramp to 100% B at 100 min and then hold to 124 min. The eluents were monitored at 254 nm and collected 0.5 min per fraction. The HS activity was observed in the eluents at retention time (Rt) 22.5-23.5 min (Fr-A1) and Rt 29.5-30 min (Fr-B1). The active fractions of Fr-A1 and Fr-B1 were then dissolved in 100 µl of chloroform/methanol (95:5) and subjected to a normal phase HPLC connected

to a YMC-Pack Diol-120-NP column (4.6 × 250 mm, 5 μm; YMC). The mobile phase consists of solvent A (chloroform) and solvent B (methanol) with flow rate at 1.0 ml min⁻¹ using linear gradient system as follows; 0% B at 0 min and hold 20 min, ramp to 10% B at 40 min and hold 50 min, 100% B at 50 min and then hold to 70 min. The eluents were monitored at 270 nm and collected 0.5 min per fraction. The HS activity was observed in the eluents at Rt 39-39.5 min (Fr-A2) and Rt 35.5-36 min (Fr-B2) derived from fraction Fr-A1 and Fr-B1, respectively.

The purified fractions were then analyzed by liquid chromatography-mass spectrometry (LC-MS) or liquid chromatography-tandem mass spectrometry (LC-MS/MS). The LC-MS System (Waters) was consisted of an AQUITY Ultra Performance Liquid Chromatograph (UPLC) H-Class System and an AQUITY quadruple tandem mass spectrometer (TQ detector). MassLynx 4.1 software (Waters) was used to perform data acquisition and analyses. Each sample was injected to an ACQUITY UPLC HSS T3 column (100 × 2.1 mm, 1.8 μm; Waters), with a column temperature of 40 °C and the flow rate of 0.2 ml min⁻¹. The mobile phase consisted of solvent A (0.1% formic acid in water) and solvent B (acetonitrile), and the gradient condition was as follows; 10% B at 0 min, ramp to 60% B at 20 min, 100% B at 20 min and hold to 25 min, and then returned to 10% B at 25min and hold to 30min. The mass spectra were obtained by positive or negative electrospray ionization (ESI) mode, with a capillary voltage of 3 kV. For the mass spectrometry scan mode, the mass range of *m/z* 100-1100 and a sample cone voltage of 25 V was used. For the SEA analysis, multiple reaction monitoring (MRM) mode was used and the MRM transitions of *m/z* 499 > 399, where a sample cone voltage of 35 V and a collision energy of 30 eV in positive ESI mode, was selected.

In order to separate two major peaks, Fr-A2 was subjected to UPLC connected to an AQUITY UPLC HSST3 column (100 × 2.1 mm, 1.8 μm) with a column temperature of 40 °C and the flow rate of 0.2 ml min⁻¹. The isocratic mode of water/acetonitrile (90:10, v/v) with 0.1 % formic acid was used. The eluents were monitored at 270 nm and collected 2 min per fraction. compound 1 and compound 2 were eluted at Rt 18-26 min and Rt 28-34, respectively. The HS activity was observed in the compound 2 eluted fractions.

Structure determination of solanoeclepin B

Due to the low amount of the active compound in the Fr-A2 (estimated to be less than 10 μg), the active compound was re-purified with an efficient method based on the detection of a novel HF with LC-MS analysis. Approximately 30 L of SP207 resin placed in potato hydroponic culture solution from June to August 2019 was packed in a column. The column was washed and eluted with three times column volumes of 20% (v/v) methanol and methanol, respectively. The methanol eluents were dried *in vacuo* and re-dissolved in 100 mL of methanol to remove methanol insoluble materials. The methanol soluble fraction (33.5 g) was dried *in vacuo*, dissolved in 200 ml of water, and treated once or twice with the same volume of n-hexane or ethyl acetate, respectively. The remaining aqueous phase was then adjusted pH 1 with 1 N HCl and extracted five times with 200 ml of ethyl acetate. The acidic ethyl acetate phase (4.3 g) was dried *in vacuo*, dissolved in 80 ml of 5% (v/v) aqueous methanol, and loaded onto Sep-Pak C18 cartridge (Vac 35 cm³, 10g) pre-washed and equilibrated with five column volumes of methanol and 5% (v/v) aqueous methanol, respectively. The cartridge was washed with five column volumes of 5% (v/v) aqueous methanol and eluted five times with one

column volume of 10, 20, 40% (v/v) aqueous methanol and subsequent five column volumes of methanol. Anyway, the 20% methanol fractions where active compound was detected were combined. The elution pattern was different among each cartridge and preliminary test due to the likely matrix effect. The combined fraction (702 mg) was subjected to silica gel column chromatography (5 g) with a stepwise elution of chloroform/methanol (100:0-50:50, 10% step, 30 ml). The active compound was eluted in chloroform/methanol (80:20) fraction (95 mg). Then, normal phase HPLC preparation was conducted as described above. The eluent at the R_t 39 min was combined (5.3 mg) and subjected to reversed phase HPLC. The reversed phase HPLC system was the same as described above, but the isocratic mode of water/methanol (85:15, v/v) with 0.05 % trifluoroacetic acid (TFA) was used instead of the gradient mode. The active compound was eluted at R_t 46min and the white powder was obtained (estimated to be 340 μg).

The LC-MS and LC-MS/MS method were as described above. For the analysis of active compound, MRM mode was used and the MRM transitions were as follows; m/z 501 > 95, 501 > 429, and 501 > 483, where a sample cone voltage of 30 V and collision energies of 30 eV for m/z 95 or 10 eV for m/z 429 and 483 in positive ESI mode were used.

The chemical formula of active compounds was estimated by trapped ion mobility time-of-flight (timsTOF) mass spectrometer (Bruker). NMR spectra were recorded on a Bruker AVANCE III 800US Plus system (Bruker) at 800 MHz for ^1H and 202 MHz for ^{13}C in deuterium oxide (D_2O ; Sigma-Aldrich). The assignments of the ^1H and ^{13}C signals were based on ^1H - ^1H correlation spectroscopy (COSY), heteronuclear single quantum coherence (HSQC), heteronuclear multiple bond correlation (HMBC),

and nuclear overhauser enhancement and exchange spectroscopy (NOESY) spectra.

HF analysis of the tomato hairy roots culture solution

Generation and cultivation condition of tomato hairy roots was as described in “Chapter 1”. Approximately 150 ml of culture solution was loaded onto a column consisting of 20 ml of Sepabeads SP207 resin. The column was washed with 20 and 60 ml of water and 20% (v/v) aqueous methanol, respectively, and eluted with 60 ml of methanol. The methanol eluents were dried *in vacuo*, re-dissolved in 100 μ l of methanol, and aliquot (10 μ l) was subjected to LC-MS/MS analysis.

Hatching assay

Hatching assay was conducted as described in “Chapter 1”.

Result

Collection of hatching factors from potato hydroponic culture solution

In order to collect and concentrate the hatching factors from bulk potato hydroponic culture solution, I used the Sepabeads SP207, the highly porous styrenic adsorbents which efficiently absorb hydrophilic organic compounds. The hatching factors were successfully absorbed to the resin and eluted with methanol (Figure 2-1). Because methanol eluents include partial water derived from the resin bed volume, the dried methanol fraction could not be completely dissolved in 100% methanol. Therefore, I separated into methanol-soluble or insoluble fraction using filter paper and hatching assay was performed with each fraction. As a result, hatching factors were highly dissolved in methanol, and thus the methanol insoluble materials could be efficiently

removed (Figure 2-1). In each following purification step, the fractions evaluated by hatching assay and found to have HS activity were used for subsequent purification. The methanol soluble fraction was then separated by liquid phase extraction. The extraction of hatching factors from the aqueous phase could be conducted by three times treatment of ethyl acetate, although the HS activity still observed in remaining water phase. In terms of the relative HS activity to fraction weight, the acidic ethyl acetate phase was further used for purification (Figure 2-2).

Separation of hatching factors using open column chromatography

I next separated acidic ethyl acetate fraction into two major fractions using Sep-Pak C₁₈ cartridge consisting of ODS resin property. The HS activity was collected almost equally in 20% aqueous methanol and 100% methanol fractions (Figure 2-3). The 100% methanol fraction was then separated by strong cation exchanger Dowex 50W resin and the major HS activity was observed in passed through fraction, suggested that the HS compounds were not cationic compound as is the same as solanoeclepin A (Figure 2-4). Next, I conducted the size exclusion column chromatography using Sephadex LH-20 resin. The HS activity was broadly collected in fractions 11 to 20, where two major peaks were observed with fraction 14 and 17 as peak top (Figure 2-5). Therefore, I separately combined fractions 11 to 16 and 17 to 20 as Frs-fast and Frs-late, respectively. Two independent fractions were then supplied to a strong anion exchange column chromatography using Dowex 1 resin. In the case of Frs-fast, the HS activity was separately collected in passed through or absorbed fraction, and the absorbed HS compounds were eluted with 1 N acetic acid methanol (Figure 2-6B). Whereas in the case of Frs-late, the HS activity was primarily absorbed to the resin (Figure 2-6C). In

terms of the relative HS activity to fraction weight, the 1 N acetic acid methanol fractions 2 and 3 derived from Frs-late were combined and used for subsequent HPLC.

Separation of hatching factors using preparative HPLC

I firstly conducted reversed phase HPLC preparation. Hatching factors were successfully absorbed to the ODS column and the HS activity was separated into two major fractions, Fr-A1 eluted at Rt 22.5-23.5 min and Fr-B1 at 29.5-30 min, respectively, suggesting the presence of at least two individual hatching factors (Figure 2-7). Each HS active fraction was then subjected to a normal phase HPLC which shows different column property and selectivity from ODS column. Hatching factors in both HS active fractions were successfully absorbed to the column and solely collected in Fr-A2 eluted at Rt 39-39.5 min and Fr-B2 eluted at Rt 35.5-36 min from Fr-A1 and Fr-B1, respectively (Figure 2-8, 2-9).

LC-MS analysis of Fr-A2 and Fr-B2

To confirm the purification level and to obtain the mass spectral information, HS active Fr-A2 and Fr-B2 were subjected to LC-MS analysis. In the case of Fr-A2, two major peaks, compound 1 and compound 2, were detected in both positive and negative ESI mode, as well as in UV chromatogram at 270 nm (Figure 2-10A-C). The major detected mass spectra of compound 1 were m/z 338.6, 356.5, 397.6, and 712.3 in positive ESI mode and m/z 354.9 in negative ESI mode, suggesting they were detected as $[M+H-H_2O]^+$, $[M+H]^+$, $[M+H+MeCN]^+$, $[2M+H]^+$, and $[M-H]^-$, respectively (Figure 2-10D). In the same case, the major mass spectra detected in compound 2 were m/z 500.7 ($[M+H]^+$) in positive ESI mode and m/z 544.9 ($[M-H+HCOOH]^-$) in negative ESI mode,

respectively (Figure 2-10E). On the other hands, a single major peak, compound 3, was detected in Fr-B2 and the detected mass spectra were m/z 498.6 and 496.7 in positive and negative ESI mode, respectively, which were identical to a previously known solanoeclepin A (Figure 2-11A-D). To confirm the presence of solanoeclepin A in Fr-B2, I compared it with synthetic solanoeclepin A using LC-MS/MS analysis. As a result, compound 3 was detected at the MRM transition channel specific for solanoeclepin A and its retention time was consistent with synthetic solanoeclepin A (Figure 2-11E).

Separation of compound 1 and compound 2 using preparative reversed-phase UPLC

Because either of compound 1 or compound 2 in Fr-A2 was suggested to be a novel hatching factor, I carried out a UPLC preparation to separate them and confirm which peak showed HS activity. LC-MS analysis indicated definite separation of two compounds. Compound 1 and compound 2 were collected between 18-26 min and 28-34 min where 20-22 min and 28-30 min were the most abundant fraction, respectively (Figure 2-12B, C). The hatching assay was then conducted. The elution pattern of compound 2 was consistent with that of HS activity (Figure 2-12D). Therefore, I identified the compound 2 as a novel hatching factor.

Structure determination of solanoeclepin B

To estimate the chemical formula of compound 2, high-resolution mass spectrometry analysis was conducted. The measured mass spectra were listed in Table 2-1 and 2-2. The prediction of a chemical formula as $C_{27}H_{32}O_9$ was in good agreement with the measured mass spectra in both ESI mode and their estimated adduct ion form. Therefore, the chemical formula of compound 2 was determined as $C_{27}H_{32}O_9$. The

chemical formula of solanoeclepin A is $C_{27}H_{30}O_9$, and compound 2 has two more hydrogen atoms, suggesting it could be a reduced structure of solanoeclepin A. The 1H -NMR spectra of compound 2 exhibited nineteen signals, which was one more signal than that of synthetic solanoeclepin A. The overall similarity of 1H -NMR spectra between compound 2 and synthetic solanoeclepin A was observed¹³. Especially, following signals were corresponding to those of synthetic solanoeclepin A in terms of chemical shifts, multiplicity, and coupling constants; two geminal protons of aliphatic methylene at δ_H 2.56 and δ_H 2.67 (H-11), and δ_H 1.47 and δ_H 2.02 (H-12), a hydroxy methine proton at δ_H 4.43 (H-15) and its adjacent geminal protons of aliphatic methylene at δ_H 2.13 and δ_H 2.27 (H-16), the characteristic high-field geminal protons at δ_H 0.95-0.91 (H-22) derived from cyclopropane ring, a hydroxy methine proton at δ_H 4.29 (H-19), a methoxy proton at δ_H 3.59 (H-27), and three methyl protons at δ_H 1.30 (H-18), δ_H 1.35, and δ_H 1.57 (H-25 and H26) (Table 2-3). These signals suggested the compound 2 shared the same partial structure with solanoeclepin A. On the other hands, although the multiplicity of a signal at δ_H 1.63 was unclear because of the overlap with other signals, the multiplicity of the signals at δ_H 1.63, δ_H 2.41, and δ_H 4.00 was different from that of synthetic solanoeclepin A. Furthermore, a signal at δ_H 4.53, which was not present in solanoeclepin A, also appeared. These signals indicated that C-2 ketone group of solanoeclepin A was substituted to C-2 hydroxy group in compound 2, supporting the above prediction that the compound 2 was a reduced structure of solanoeclepin A. Thus, the hydroxy methine proton at δ_H 4.53 (H-2) was observed in compound 2 as well as the coupling with 1.63, δ_H 2.41 (H-1), and δ_H 4.00 (H-3) (Table 2-3). Since the solanoeclepin A is a sure HS active compound with a highly complex structure and 1H -NMR spectra of compound 2 showed overall similarity to

solanoeclepin A, I expected the HS active compound 2 to have a structure almost identical to that of solanoeclepin A, only with the C-2 ketone group substituted to a hydroxy group (Figure 2-13). The observed spectra of ^1H - ^1H COSY, HSQC, and HMBC supported the estimated structure, although five carbon signals at C-7, C-14, C-17, C-20, and C-24 were missing because I couldn't obtain the favorable ^{13}C -NMR spectra due to the low amount of compound 2 (Figure 2-14, Table 2-3). The coupling constant between H-2 and H-3 were similar to that of compound a, not compound b, indicated the stereochemistry of C-2 to be *R* configuration^{32,33} (Figure 2-15). Therefore, the structure of a novel hatching factor was established to be (1*R*,2*R*)-2-[(1*R*,7*R*,8*R*,10*R*,11*S*,15*S*,16*R*,18*S*)-3,19-dioxo-4-methoxy-8,11,18-trihydroxy-6,6,15-trimethyl-20-oxahexacyclo[14.2.1.1^{7,10}.0^{1,15}.0^{2,12}.0^{5,10}]icosa-2(12),4-dien-16-yl]cyclopropane-1-carboxylic acid, and is assigned the name as solanoeclepin B (SEB).

Presence of SEB in tomato hairy root culture solution.

In order to detect the SEB with unpurified samples, I developed the analytical method using LC-MS/MS analysis. The observed product ion spectra of SEB using collision induced dissection with the collision energy ranging from 10 eV to 50 eV were shown in Figure 2-16A. Based on them, I established the MRM transition mode of m/z 501 > 429 (Figure 2-16B). In tomato hairy roots culture solution, the peak which showed the identical retention time to SEB was detected (Figure 2-17). In contrast, SEA was not detected from tomato hairy roots culture solution. These results suggesting the SEB, not SEA, was the major HF produced by tomato hairy roots.

Discussion

In this chapter, I conducted the purification of HFs from bulk potato hydroponic culture solution and successfully obtained a pure HS active compound, SEB, and determined its structure. In addition to SEB, SEA was also detected in potato hydroponic culture solution. There are still several HS active fractions without further purification in this study. In these HS active fractions such as 20% methanol fraction in Sep-Pak C₁₈ purification step or 1N AcOH fractions derived from Frs-fast in Dowex 1 purification step, SEB was also detected and suggested to be covered the observed HS activity. On the other hands, SEB was not detected in the HS active fraction of Dowex 1 passed through fraction derived from Frs-fast. Consequently, SEA and SEB are the major active HFs in potato hydroponic solution, although the presence of other unidentified HFs is possible. In the case of tomato, SEB was detected from tomato hairy roots culture solution, but SEA was not. Recently, Guerrieri et al. reported the detection of SEA from passed through water of soil where tomatoes were grown³⁴. Since the tomato hairy roots culture system is in aseptic whereas the soil condition is quite complex due to the soil microorganisms, pH, and moisture, the HF production in potato and tomato could be affected and fluctuated.

In comparison with the structure of SEA and SEB, there is a difference at C-2 ketone or hydroxy group. In addition, C-2 group of glycinoclepin A, B, and C, which showed the HS activity toward the soybean cyst nematode (SCN) eggs, are not substituted with ketone or hydroxy group^{9,10}. Accordingly, it is suggested that the structural requirement of HS activity is not included in C-2, although further studies were needed.

In conclusion, I identified a novel HF, SEB, which is present in both potato and tomato root exudates. The SEB is detectable from laboratory-scale tomato hairy roots culture system, allowing us detail investigation of HF biosynthesis using SEB analytical method.

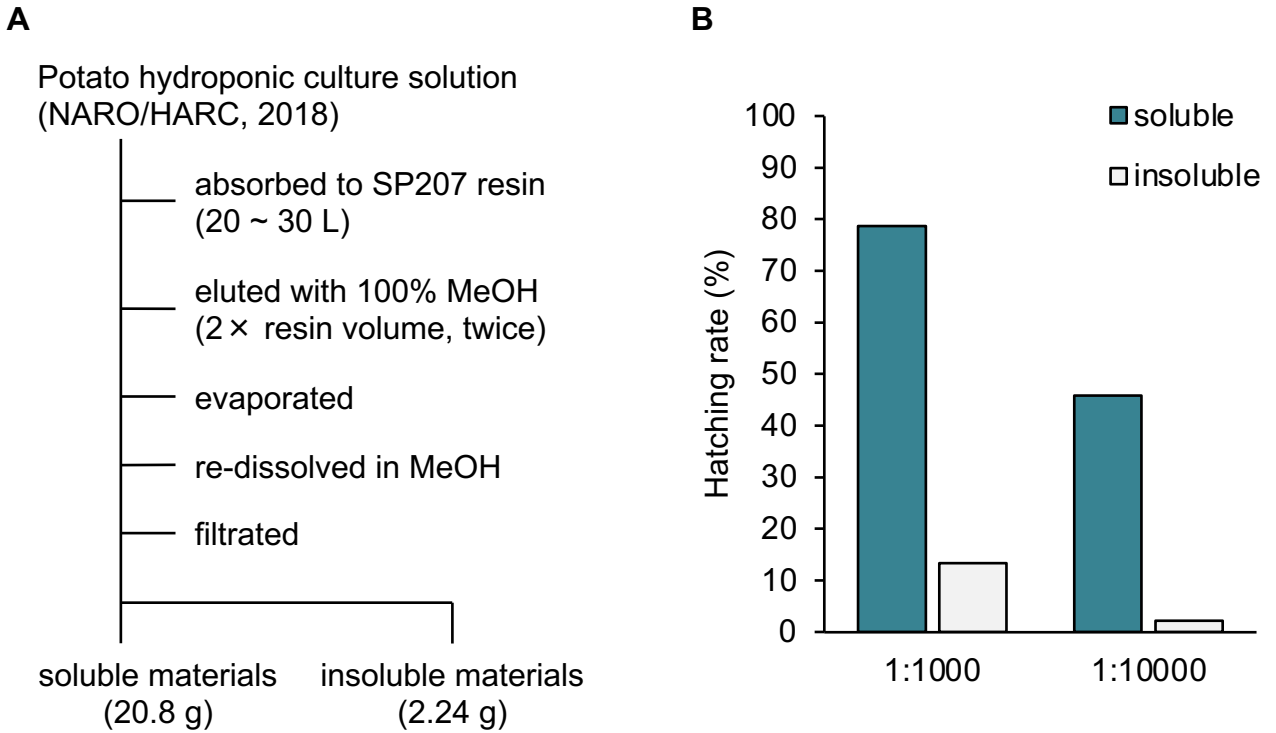


Figure 2-1. Concentration of hatching factors from potato hydroponic culture solution. (A) Schematic concentration process using Sepabeads SP207 resin. (B) Hatching stimulation activity of the methanol eluents from Sepabeads SP207 resin. Hatching assay was conducted with Gr eggs. The hatching rates (%) are shown at two dilution series.

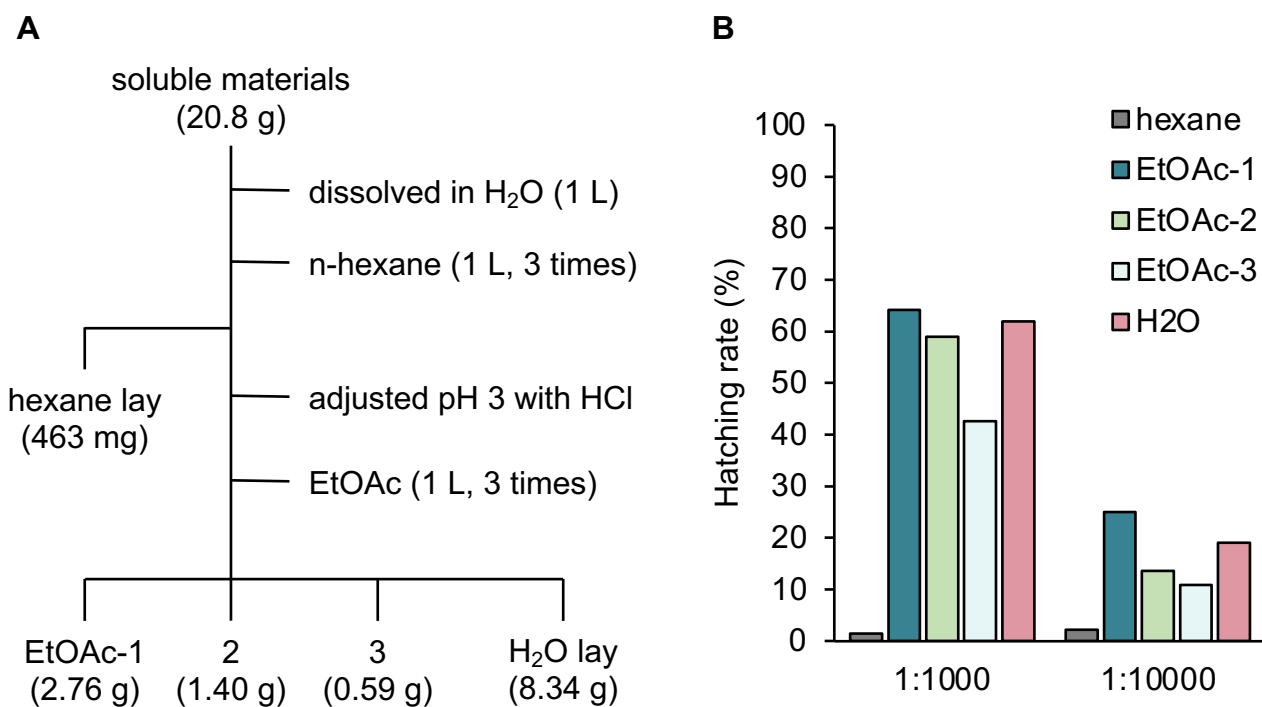


Figure 2-2. Liquid phase extraction of hatching factors.

(A) Schematic process of liquid phase extraction. (B) Hatching stimulation activity of n-hexane, ethyl acetate, and aqueous phase. Hatching assay was conducted with Gr eggs. The hatching rates (%) are shown at two dilution series.

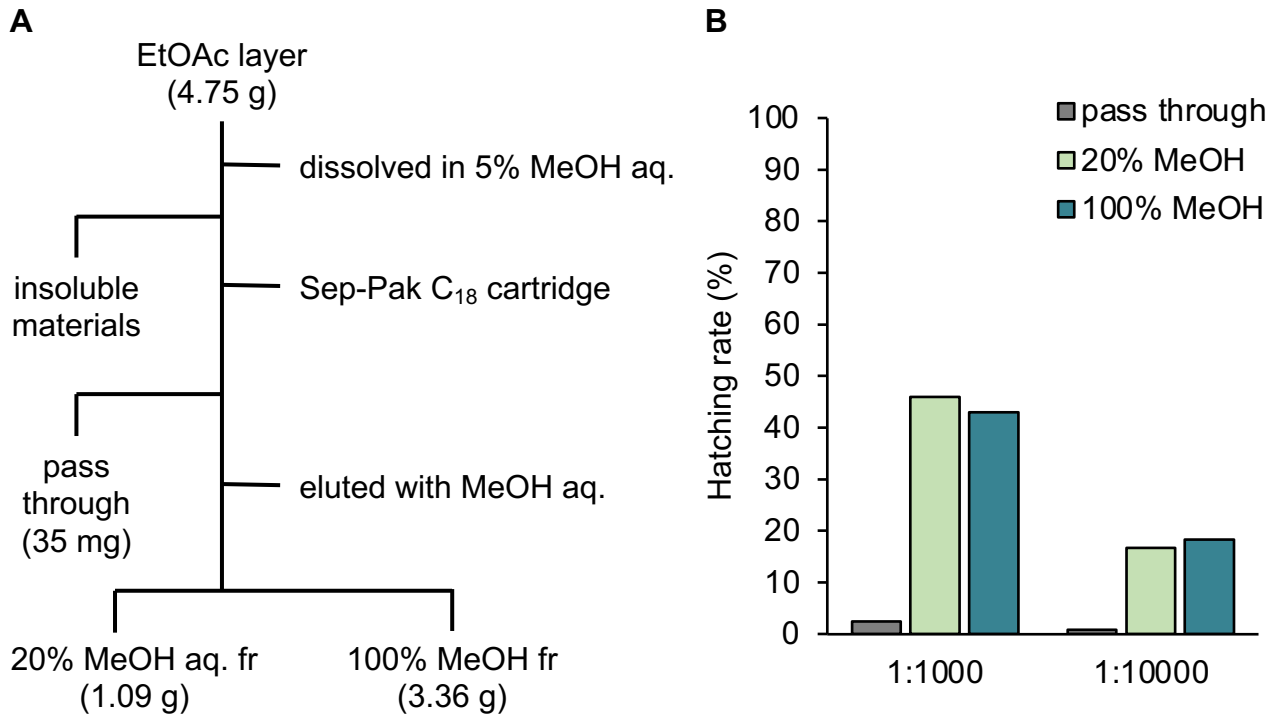


Figure 2-3. Separation of hatching factors using ODS column chromatography.

(A) Schematic process of ODS column chromatography. (B) Hatching stimulation activity of each separated fraction. Hatching assay was conducted with Gr eggs. The hatching rates (%) are shown at two dilution series of methanol-soluble or -insoluble fraction, respectively.

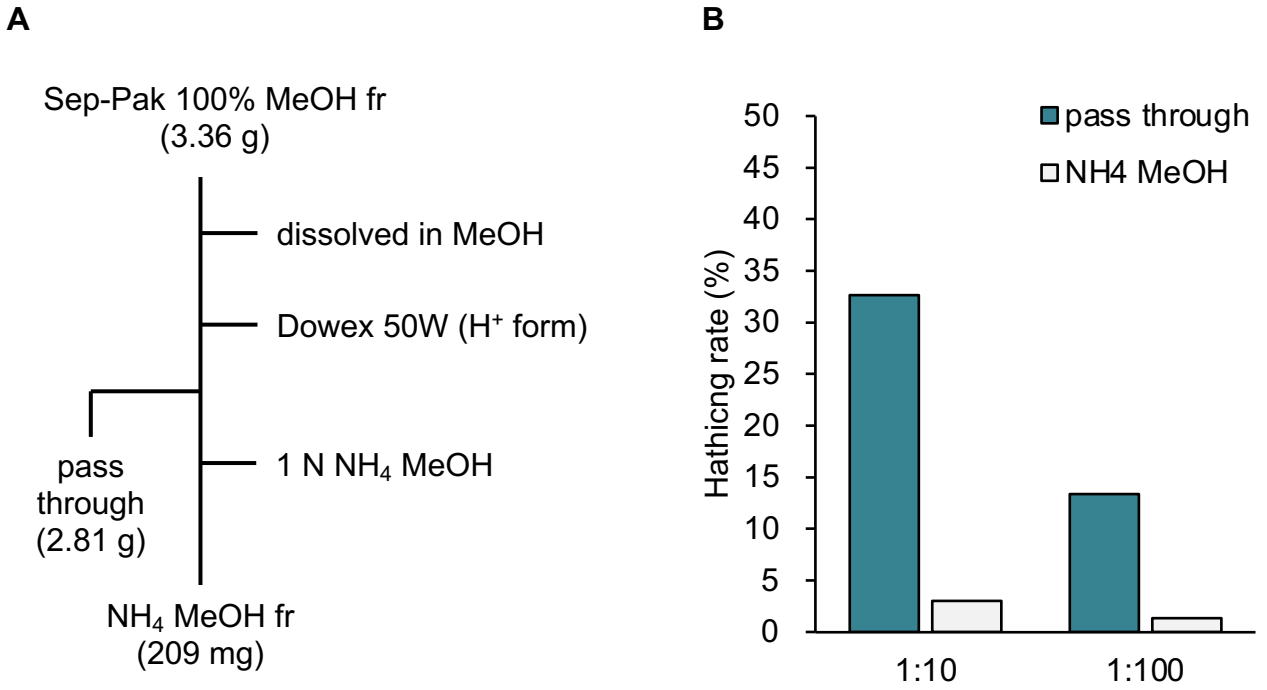


Figure 2-4. Separation of hatching factors using strong cation exchange (SCX) column chromatography.

(A) Schematic process of SCX column chromatography. (B) Hatching stimulation activity of each separated fraction. Hatching assay was conducted with Gr eggs. The hatching rates (%) are shown at two dilution series.

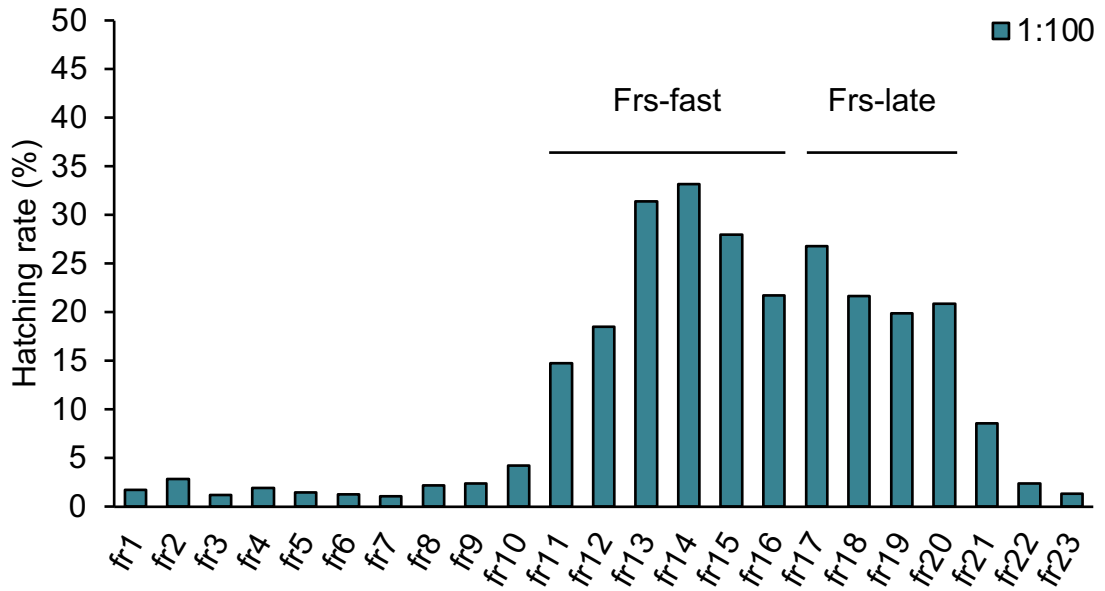


Figure 2-5. Separation of hatching factors using size exclusion column chromatography. Hatching stimulation activity of each separated fraction. Hatching assay was conducted with Gr eggs. The hatching rates (%) are shown at one point of dilution (1:100)

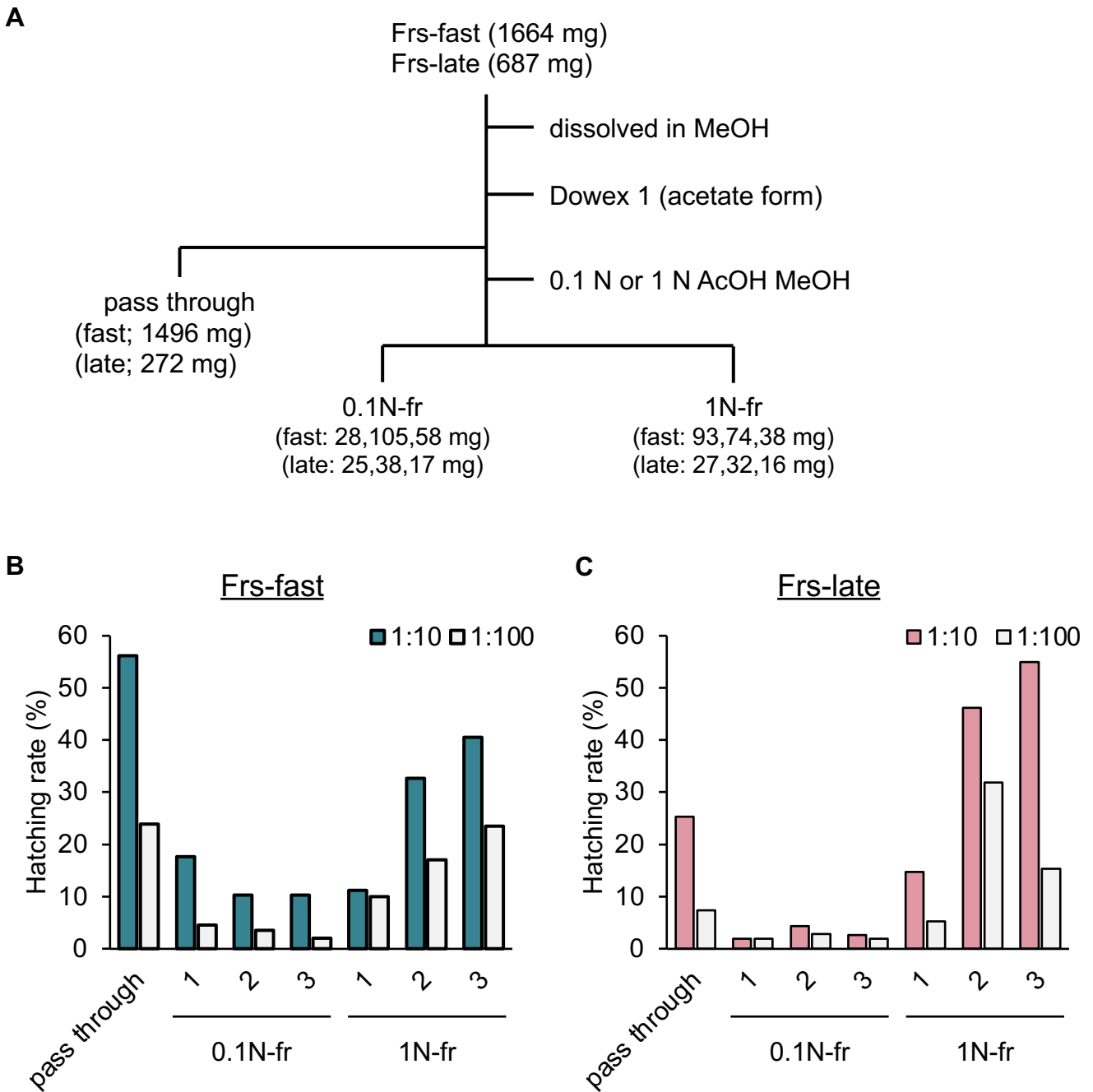


Figure 2-6. Separation of hatching factors using strong anion exchange (SAX) column chromatography.

(A) Schematic process of SAX column chromatography. (B,C) Hatching stimulation activity of each separated fraction derived from Frs-fast (B) and Frs-late (C). Hatching assay was conducted with Gr eggs. The hatching rates (%) are shown at two dilution series.

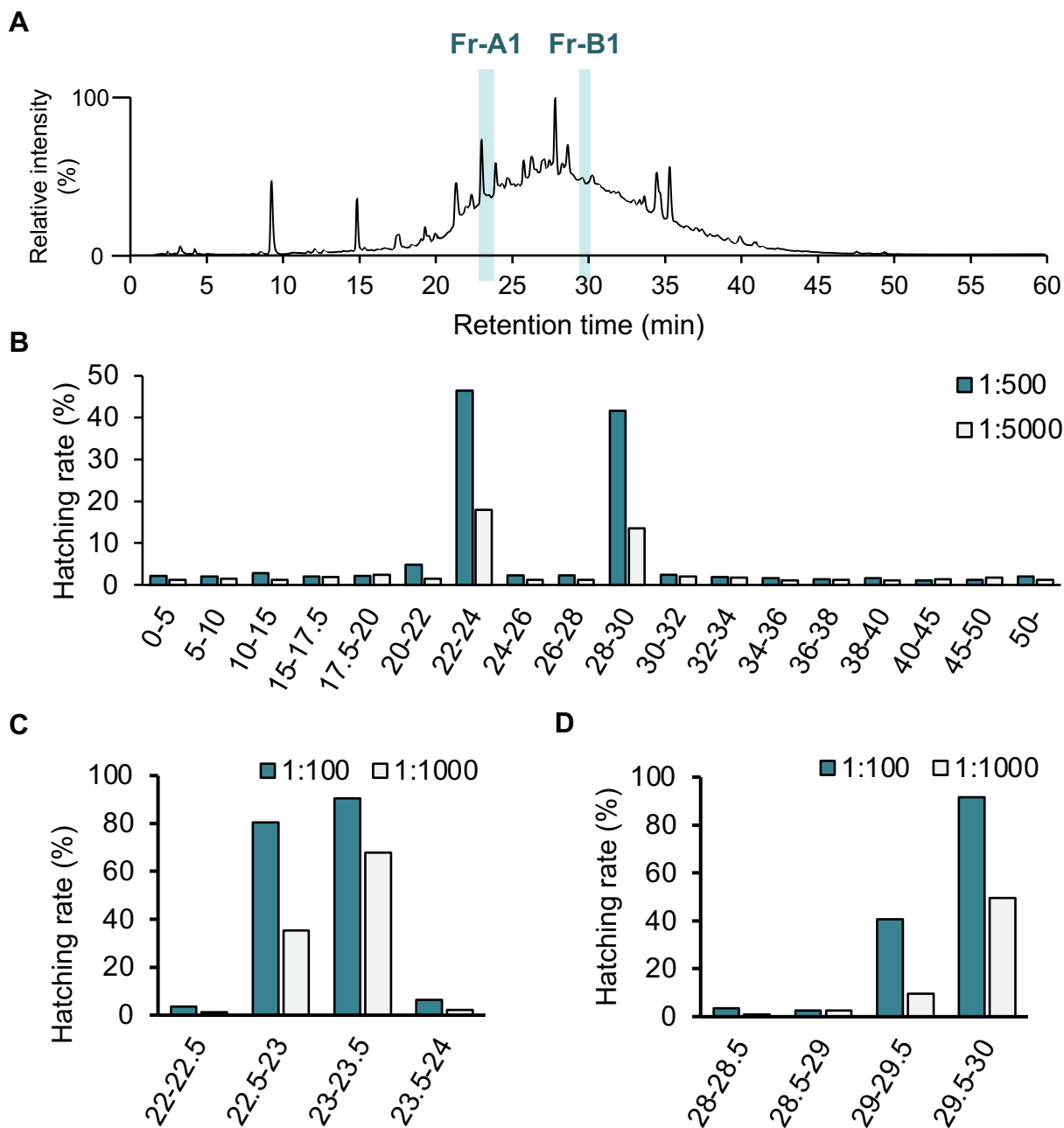


Figure 2-7. Separation of hatching factors using preparative ODS-HPLC.

(A) A chromatogram of UV absorbance at 254 nm is shown. (B-D) Hatching stimulation activity of fractions collected during each retention times. Hatching assay was conducted with Gr eggs. The hatching rates (%) are shown at two dilution series. Fractions were grouped and tested at first (B) and then each fraction in the group of 22-24 min (C) and 28-30 min (D) observed hatching stimulation activity was tested independently.

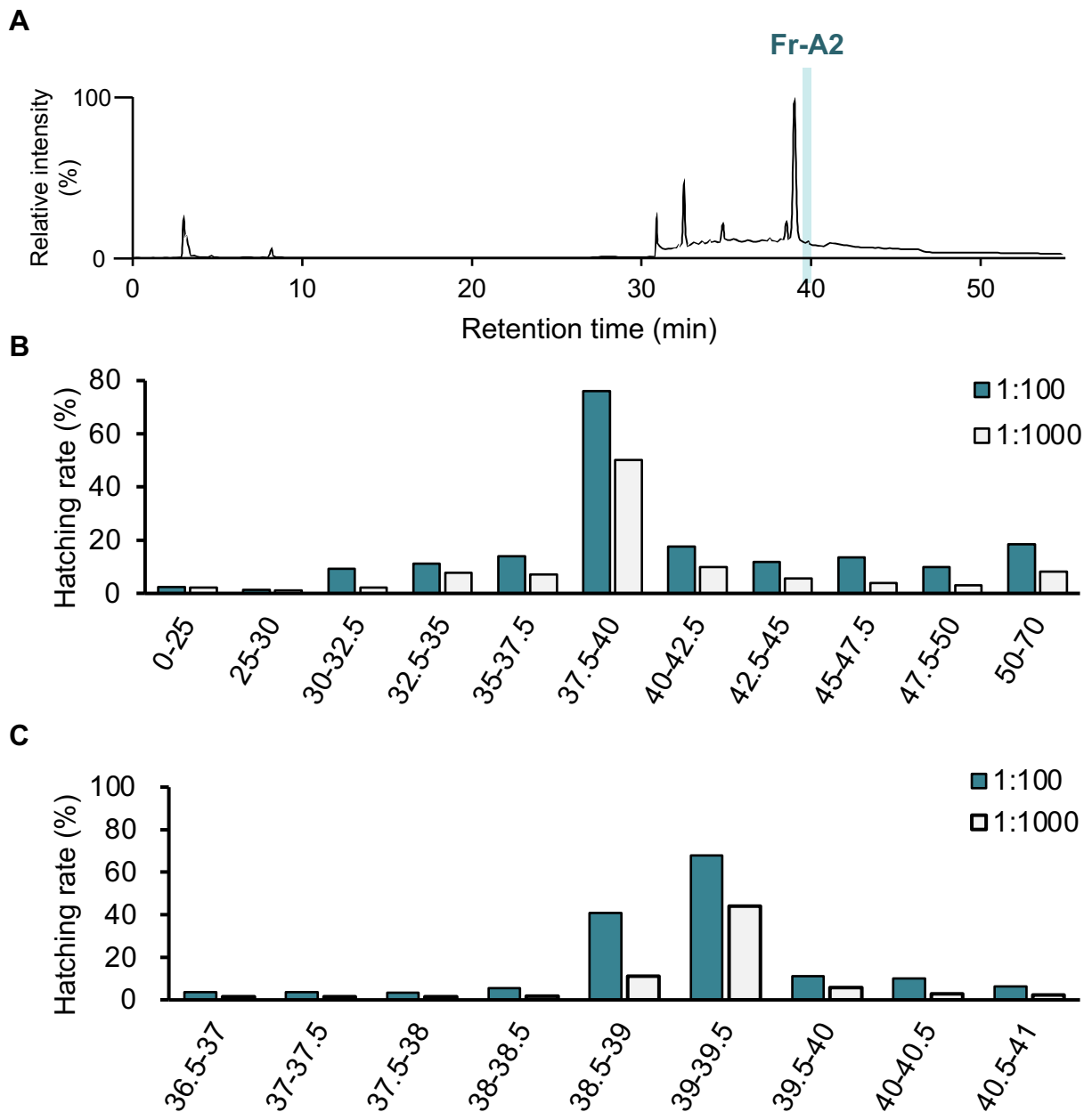


Figure 2-8. Separation of hatching factors in Fr-A1 using preparative NP-HPLC.

(A) A chromatogram of UV absorbance at 270 nm is shown. (B, C) Hatching stimulation activity of fractions collected during each retention times. Hatching assay was conducted with Gr eggs. The hatching rates (%) are shown at two dilution series. Fractions were grouped and tested at first (B) and then each fraction around the group of 37.5-40 min observed hatching stimulation activity was tested independently (C).

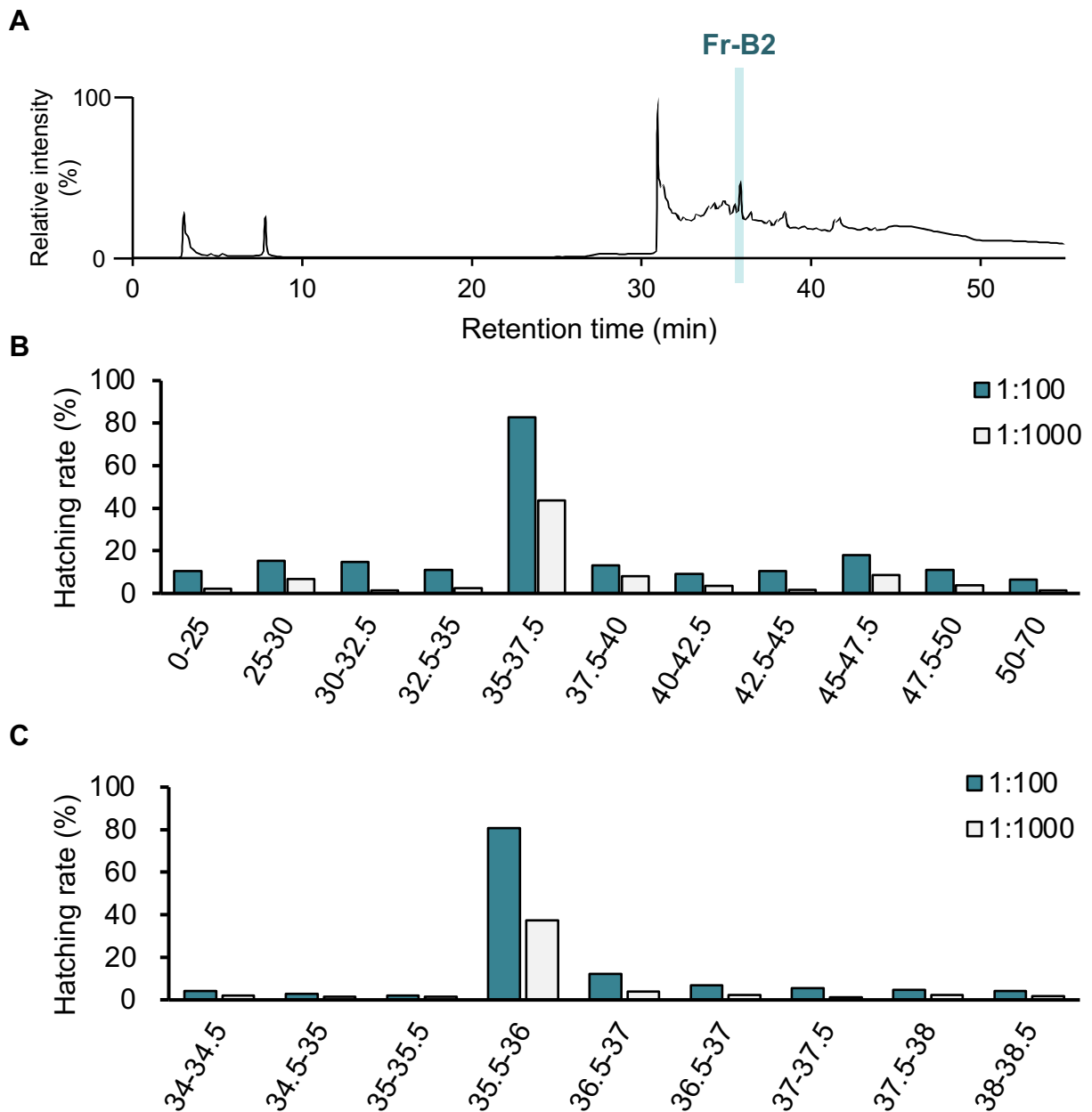


Figure 2-9. Separation of hatching factors in Fr-B1 using preparative NP-HPLC.

(A) A chromatogram of UV absorbance at 270 nm is shown. (B, C) Hatching stimulation activity of fractions collected during each retention times. Hatching assay was conducted with Gr eggs. The hatching rates (%) are shown at two dilution series. Fractions were grouped and tested at first (B) and then each fraction around the group of 35-37.5 min observed hatching stimulation activity was tested independently (C).

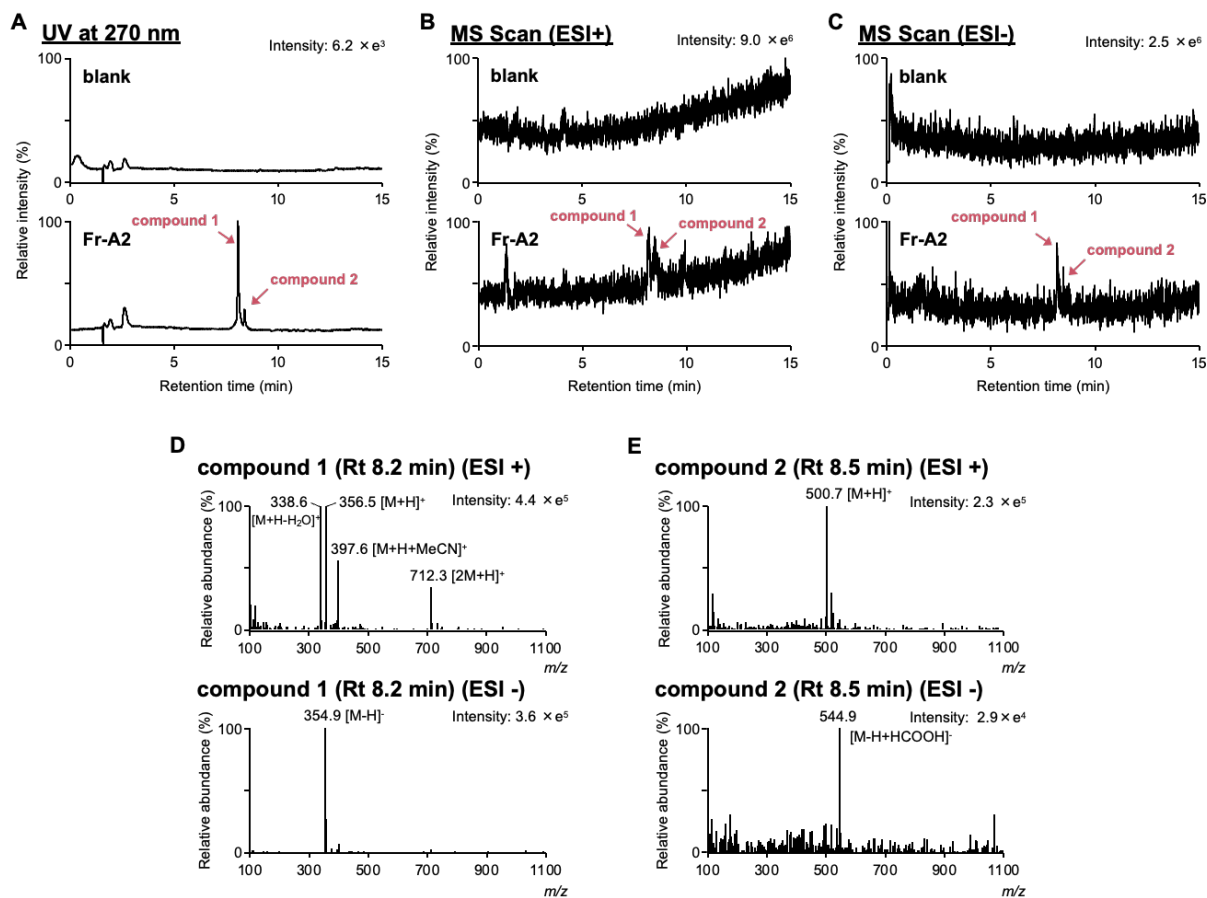


Figure 2-10. LC-MS analysis of Fr-A2.

(A) Chromatograms of UV absorbance at 270 nm are shown. (B, C) Chromatograms obtained by positive (B) and negative (C) ESI mass spectrometry scan mode with the range of m/z 100-1100 are shown. (D, E) Positive and negative ESI mass spectra obtained at Peak 1 (Rt 8.2 min) (D) and Peak 2 (Rt 8.5 min) (E) are shown.

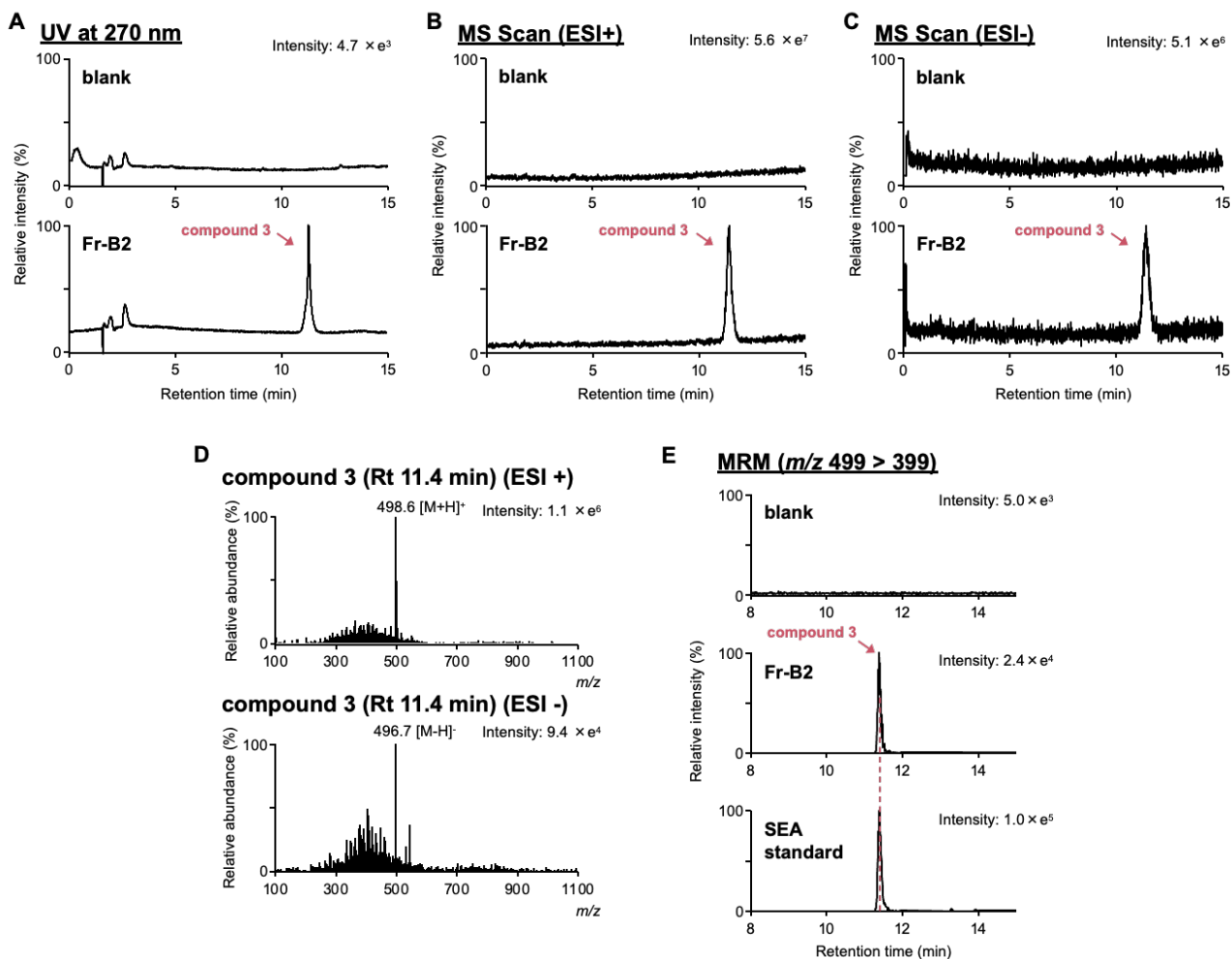


Figure 2-11. LC-MS analysis of Fr-B2.

(A) Chromatograms of UV absorbance at 270 nm are shown. (B, C) Chromatograms obtained by positive (B) and negative (C) ESI mass spectrometry scan mode with the range of m/z 100–1100 are shown. (D) Positive and negative ESI mass spectra obtained at Peak 3 (Rt 11.4 min). (E) MRM chromatograms of Fr-B2 and SEA standard. A MRM transition of m/z 499 > 399 was selected for detecting SEA.

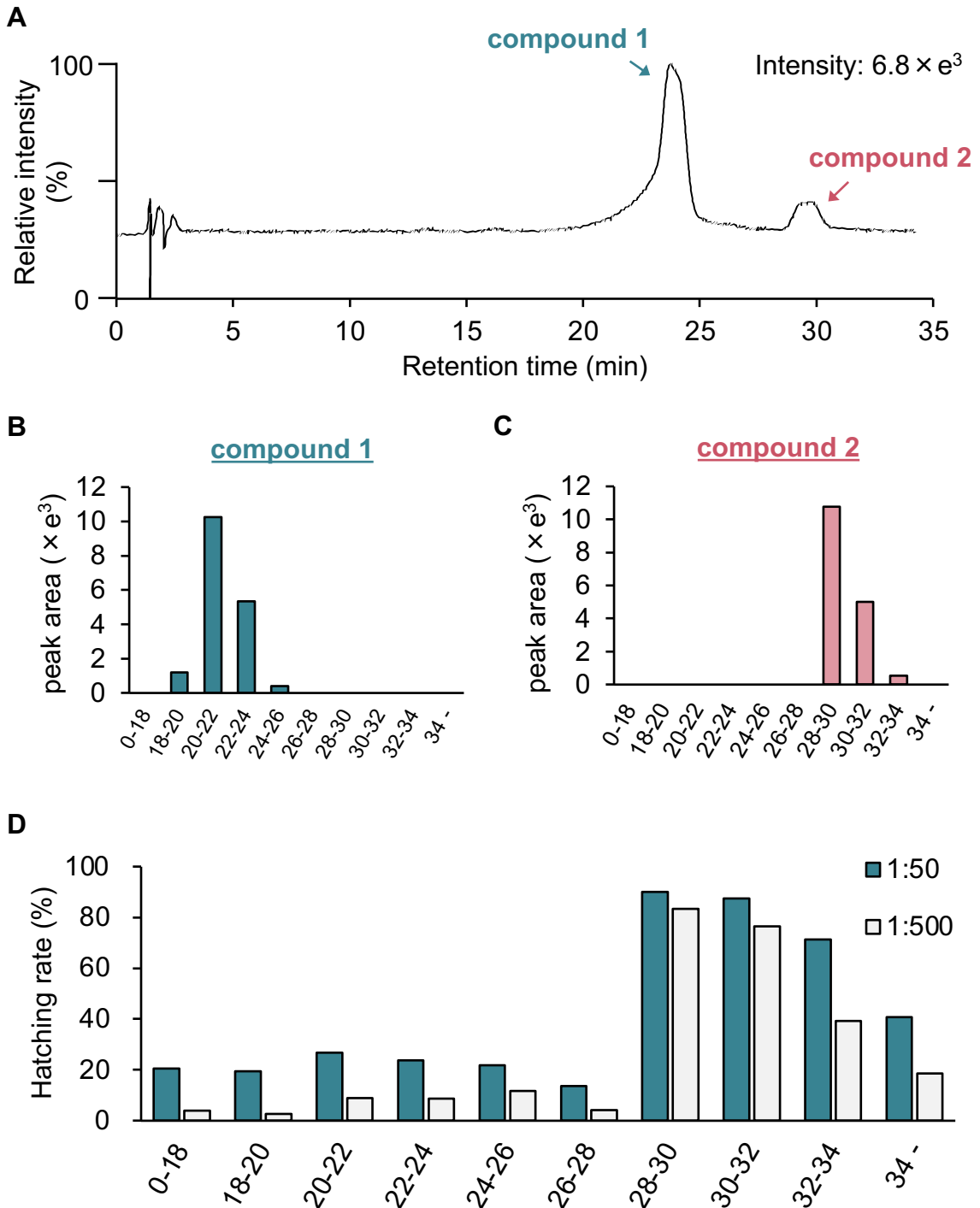
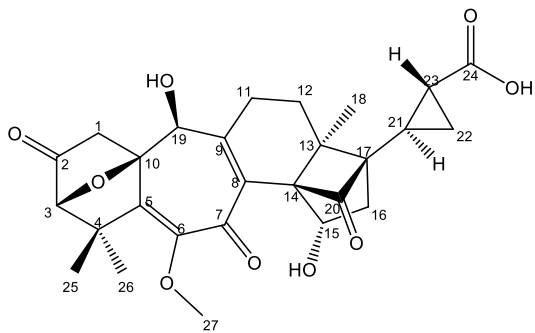
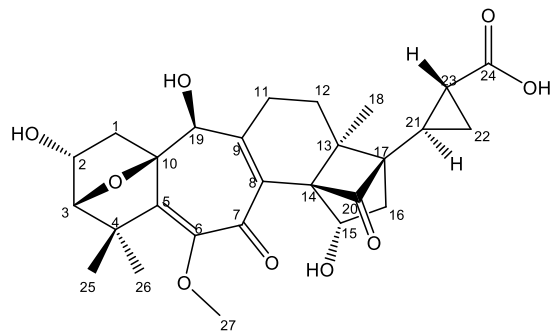


Figure 2-12. Separation of Peak 1 and Peak 2 in Fr-A2 using preparative UPLC.

(A) A chromatogram of UV at 270 nm is shown (B, C) Quantification of Peak 1 (B) and Peak 2 (C) in each separated fraction using LC-MS analysis. (D) Hatching stimulation activity of fractions collected during each retention times. Hatching assay was conducted with Gr eggs. The hatching rates (%) are shown at two dilution series.



solanoeclepin A (SEA)



solanoeclepin B (SEB)

Figure 2-13. Structure of SEA and estimated structure of SEB.

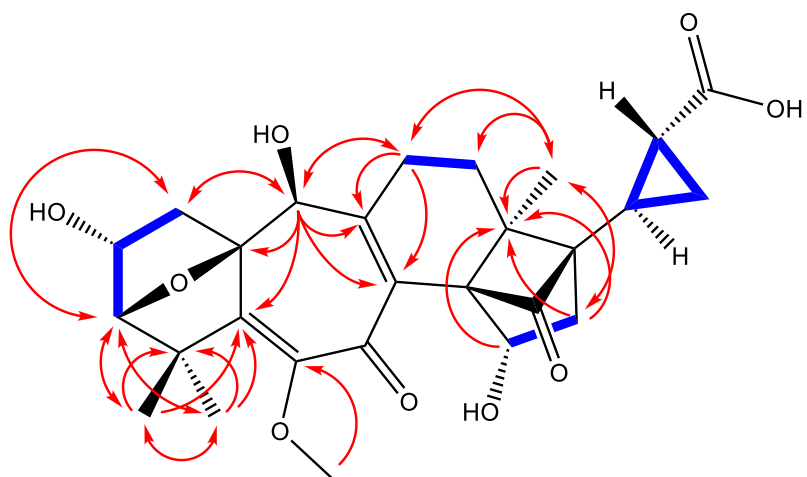
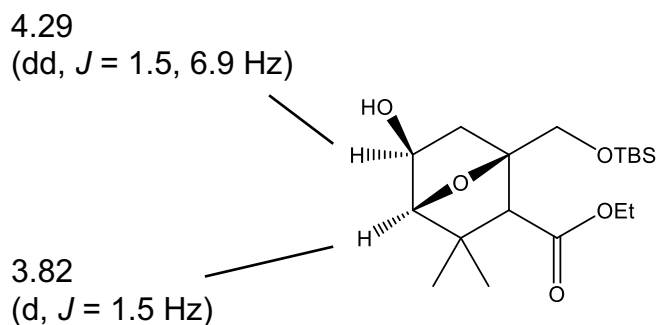
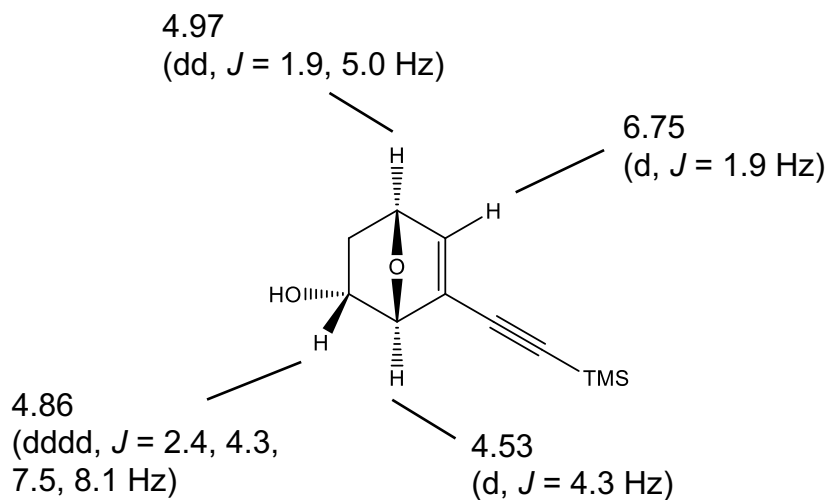


Figure 2-14. Observed COSY (blue bold bond) and HMBC (red arrow) of SEB.



compound a

(+)-(1*R*,2*S*,4*R*,5*S*)-1-(tert-Butyldimethylsilyloxymethyl)-5-hydroxy-3,3-dimethyl-7-oxabicyclo[2.2.1]heptane-2-carboxylic acid ethyl ester



compound b

(±)-6-[(Trimethylsilyl)ethynyl]-7-oxabicyclo[2.2.1]hept-5-en-2-endo-ol

Figure 2-15. ^1H chemical shifts and coupling constants of structurally related compounds

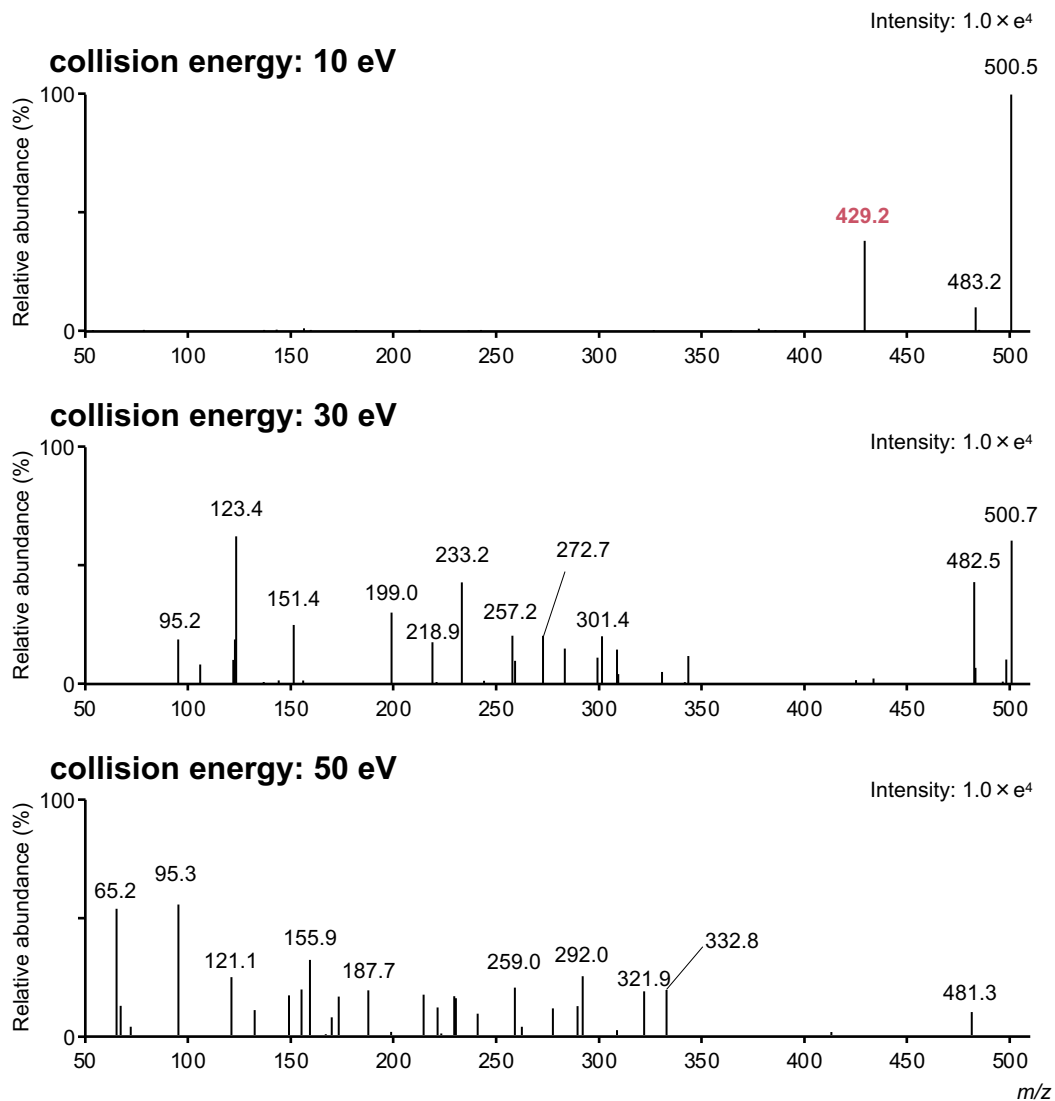
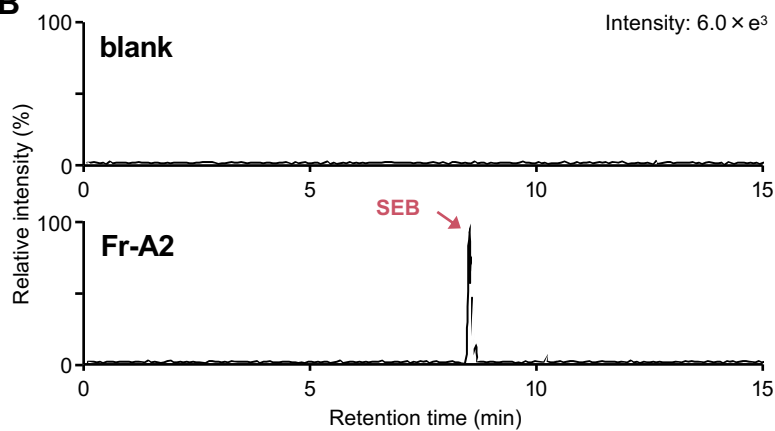
A**B**

Figure 2-16. Method construction for detecting HF-500 using LC-MS/MS analysis. (A) Product ion spectra ranging with 10 eV to 50 eV are shown. (B) MRM chromatograms of Fr-A2. A MRM transition of m/z 501 > 429 were selected.

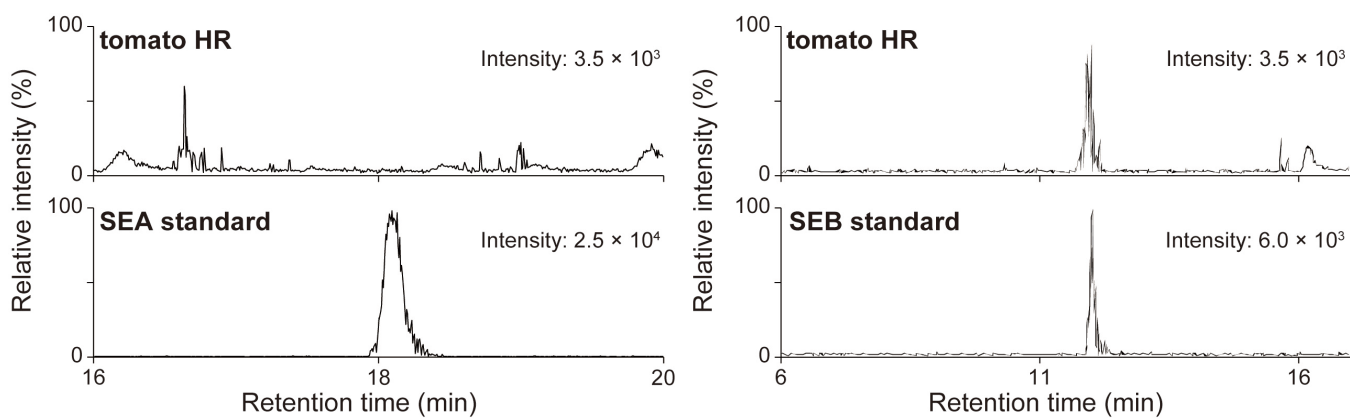


Figure 2-17. Hatching factor in tomato hairy root culture solution.

The chromatograms obtained by MRM transition channel of m/z 499 > 399 and m/z 501 > 429 for SEA and SEB, respectively.

Table 2-1. Ion formula of HF-500 estimated by positive ESI HRMS analysis.

<i>m/z</i> (measured)	Estimated ion formula	<i>m/z</i> (calculated)	Error (ppm)	Ion type
501.2118	C ₂₇ H ₃₃ O ₉	501.2119	0.3	[M+H] ⁺
	C ₂₈ H ₂₉ N ₄ O ₅	501.2132	2.9	-
	C ₂₄ H ₂₅ N ₁₀ O ₃	501.2106	-2.4	-
523.1940	C ₂₇ H ₃₂ NaO ₉	523.1939	-0.2	[M+Na] ⁺
	C ₂₈ H ₂₉ N ₄ O ₅	523.1952	2.3	-
	C ₂₄ H ₂₅ N ₁₀ NaO ₃	523.1925	-2.8	-
539.1681	C ₂₇ H ₃₂ KO ₉	539.1678	-0.5	[M+K] ⁺

Table 2-2. Ion formula of HF-500 estimated by negative ESI HRMS analysis.

<i>m/z</i> (measured)	Estimated ion formula	<i>m/z</i> (calculated)	Error (ppm)	Ion type
499.1969	C ₂₇ H ₃₁ O ₉	499.1974	0.9	[M-H]-
	C ₂₈ H ₂₈ N ₄ O ₅	499.1987	3.6	-
545.2031	C ₂₈ H ₃₃ O ₁₁	545.2028	-0.6	[M-H+HCOOH]-
559.2160	C ₂₉ H ₃₅ O ₁₁	559.2185	4.4	[M-H+CH ₃ COOH]-

Table 2-3. ¹³C and ¹H assignments of SEB and SEA.

position	solanoeclepin B				solanoeclepin A		
	δ_C	δ_H	multiplicity	coupling constant	δ_H	multiplicity	coupling constant
1	41.85	1.63	1H ^a		2.46	1H, d	$J = 17.2$ Hz
		2.41	1H, dd	$J = 12.3, 10.5$ Hz	2.55	1H, d	$J = 17.2$ Hz
2	74.85	4.53	1H, ddd	$J = 14.6, 4.3, 4.3$ Hz			
3	87.62	4.00	1H, d	$J = 4.8$ Hz	4.01	1H, s	
4	52.38						
5	154.68						
6	146.81						
7	- ^d						
8	150.55						
9	132.68						
10	93.48						
11	32.21	2.56	1H, dd	$J = 20.0, 5.4$ Hz	2.42	1H, dd	$J = 19.8, 5.0$ Hz
		2.67	1H, ddd	$J = 20.1, 11.6, 5.7$ Hz	2.53	1H, ddd	$J = 19.8, 6.0, 5.8$ Hz
12	33.65	1.47	1H, ddd	$J = 12.9, 12.9, 5.8$ Hz	1.71–1.67	1H, m	
		2.02	1H, dd	$J = 14.0, 5.5$ Hz	1.89	1H, dd	$J = 14.3, 4.6$ Hz
13	39.9						
14	- ^c						
15	66.88	4.43	1H, dd	$J = 7.8, 3.0$ Hz	4.27	1H, dd	$J = 7.4, 3.0$ Hz
16	39.76	2.13	1H, dd	$J = 12.6, 3.0$ Hz	1.97	1H, dd	$J = 12.6, 3.0$ Hz
		2.27	1H, dd	$J = 12.4, 7.6$ Hz	2.1	1H, dd	$J = 12.6, 7.4$ Hz
17	- ^c						
18	15.08	1.30	3H, s		1.14 ^b	3H, s	
19	75.6	4.29	1H, s		4.38	1H, s	
20	- ^c						
21	17.99	1.32	1H, m		1.42-1.31	1H ^a	
22	11.99	0.95- 0.91	2H, m		1.03–0.96	2H, m	
23	21.4	1.63	1H ^a		1.42-1.31	1H ^a	
24	- ^c						
25, 26	28.31	1.35	3H, s		1.15 ^b	3H, s	
		24.17	1.57	3H, s		1.28	3H, s
27	62.54	3.59	3H, s		3.42	3H, s	

a: overlapping

b: unable to distinguish

c: could not detect

Chapter 3

Identification of the oxygenase genes involved in solanoeclepin B biosynthesis from tomato

Introduction

As described in “General introduction”, solanoeclepin A (SEA) is the only natural compound that has been identified as a hatching factor (HF) toward potato cyst nematode (PCN) eggs. In addition to SEA, I have successfully identified solanoeclepin B (SEB) which is a similar structure of SEA, from potato hydroponic culture solution, and SEB was detected in tomato hairy root culture solution in “Chapter 2”. SEA and SEB, also glycinoclepin A, B, and C, are classified as triterpenoids, and their biosynthetic pathways are thought to be originated from 2,3-oxidosqualene, a common precursor of triterpenoids. However, HF biosynthesis has not been investigated to date.

In this chapter, I investigate the SEB biosynthesis using a tomato hairy root culture system by focusing on two oxygenases, cytochrome P450 monooxygenase (CYP) and 2-oxoglutarate dependent dioxygenase (DOX) which are generally involved in triterpenoid biosynthesis. The genome editing experiments, in which candidate biosynthetic genes were disrupted by CRISPR/Cas9 system, resulted in the decrease of HS activity as well as the disappearance of SEB in tomato hairy roots. Taken together, these five genes encoding oxygenase were identified as biosynthetic gene involved in the solanoeclepin biosynthesis.

Materials and methods

Chemicals

Uniconazole P and prohexadione were purchased by Wako.

Plant materials

The tomato plant used in this chapter was *S. lycopersicum* cv Micro-Tom (TOMJPF00001). For the hydroponic cultivation of tomato, the surface-sterilized seeds of tomato were germinated and cultivated under the condition of 25°C with 16/8-h light/dark photoperiod on Jiffy-7 pellets (Sakata Seed) for 2 weeks. Then, seedlings were transferred to the 500 ml bottles and grown hydroponically for 6 weeks in 1/2 Hoagland nutrient solution exchanging every 2 weeks. For the preparation of hatching assay samples, 100 mg of each tissue from fresh plant material was frozen and homogenized with a mixer mill at 4°C. The homogenates were extracted three times with 1 ml of methanol. After centrifugation, the supernatant was collected, dried in vacuo, and re-dissolved in 1 ml of water. In the case of root exudates, aliquots of the hydroponic culture solution were freeze-dried and the hatching assay samples were prepared as the amount of hydroponic culture solution corresponding to 100 mg fresh weight roots in 1 ml of water. The remaining solutions were stored at 4°C until the hatching factor extraction.

Inhibitor treatment

The generation and the cultivation condition of tomato hairy roots were as described in chapter 1. Two-weeks-old tomato hairy roots cultivated in liquid B5 medium were transferred to another 50 ml of liquid B5 medium supplemented with 50 µl of 1 or 100

mM inhibitor (uniconazole P or prohexadione) in acetone solution to give final concentrations of 1 or 100 μ M. The medium supplemented with 50 μ l of acetone was prepared as the mock treatment. After 3 days cultivation at 25°C, each 10 ml of culture solution was harvested and stored at -30°C until the hatching factor extraction.

Extraction of plant DOX sequences

Tomato amino acid sequences and the tissue specific RNA-seq data were obtained from Sol Genomics Network (<https://solgenomics.net/>). Amino acid sequences of potato (*S. tuberosum*), *Arabidopsis thaliana*, and Rice (*Oryza sativa*) were obtained from Spud DB potato genomics resource (<http://potato.plantbiology.msu.edu/>), The Arabidopsis Information Resource (TAIR; <https://www.arabidopsis.org/>), and PlantGDB (<https://www.plantgdb.org/>), respectively. Amino acid sequences of soybean (*Glycine max*), kidney bean (*Phaseolus vulgaris*), and *Lotus japonicus* were obtained from Legume Information System (<https://legumeinfo.org/>). The BLASTP search was performed against the amino acid sequences previously classified as DOX³⁵.

Construction of phylogenetic tree of plant DOXC20 family

A phylogenetic tree was constructed using the MEGA10 program and the maximum likelihood method with the following parameters: Poisson correction, pairwise deletion.

Construction of CRISPR/Cas9 vectors

The tomato hairy roots knocking out each of *SIDOX60*, *SIDOX70*, *SIDOX80*, *SICYP749A19*, and *SICYP749A20* were generated by targeted genome editing with the CRISPR/Cas9 system²⁴. I used the CRISPR/Cas9 binary vector pMgP237-2A-GFP to

express multiplex guide RNAs (gRNAs). To design a gRNA target with low off-target effect, *in silico* analyses were conducted using by the Web tool Design sgRNAs for CRISPRko (<https://portals.broadinstitute.org/gpp/public/analysis-tools/sgrna-design>) and CasOT software³⁶. Three target sequences were selected for each gene (Figure 3-2 to 3-6). To enhance the efficiency of gRNA transcription from U6 promoter, one G was added to the 5'- end of SIDOX860_guide3, SIDOX870_guide1, SIDOX870_guide2, SIDOX870_guide3, SIDOX980_guide1, SIDOX980_guide2, SIDOX980_guide3, SICYP749A19_guide1, SICYP749A20_guide1, SICYP749A20_guide2, and SICYP749A20_guide3. Two DNA fragments composed of the gRNA scaffold and tRNA scaffold between full sequence of guide 1 and partial sequence from 5'- end of guide 2, and remained partial sequence of guide 2 and full sequence of guide 3 were generated by PCR using pMD-gtRNA containing gRNA and tRNA scaffolds as a template and primer sets containing restriction enzyme BsaI sites (in the case of *SIDOX70* as a target gene, Primer-1 and Primer-3, or Primer-2 and Primer-4 were used to generate former or latter units, respectively) (Table 3-1). Each unit containing gRNA-tRNA was co-inserted into the BsaI site of pMgP237-2A-GFP using Golden Gate Cloning method to construct the CRISPR/Cas9 vectors.

Genotyping of the transgenic hairy roots

The CRISPR/Cas9 vectors of each target gene were independently introduced into *Agrobacterium rhizogenes* ATCC15834 by electroporation. Generation of the transgenic tomato hairy roots was as described in “Chapter 1”. Genome DNA was extracted from each established hairy root using DNeasy Plant Mini Kit (Qiagen). To analyze the mutations in the transgenic hairy roots, the region including the target sites of gRNAs

was amplified by PCR and the primer was listed in Table 3-1. Each PCR fragment was cleaned using the Wizard SV Gel and PCR Clean-Up System (Promega), and cloned into pCR4Blunt-TOPO (Invitrogen). Sanger sequencing of each of the cloned DNAs was performed using a sequencing service (Eurofins Genomics).

Phytohormone treatment

For gene expression analysis, 50 µl each of 100 mM methyl jasmonate (MeJA), methyl salicylate (MeSA), abscisic acid (ABA), or gibberellic acid 3 (GA3) and 20 mM of indole-3-acetic acid (IAA) or *trans*-zeatin (tZ) in methanol solution, respectively, was administered onto 5-days-old tomato hairy roots cultivated in 20 ml of liquid B5 medium. For the mock treatment, 50 µl of methanol was administered onto the medium. After 12 hours incubation, hairy roots were harvested. For the preparation of hatching assay samples, phytohormone treatment was conducted with the same method as described in “***Inhibitor treatment***”, and each culture solution cultivated for 3 days was harvested and used for hatching assay.

RNA-seq analysis

RNeasy Plant Mini Kit (Qiagen) and the RNase-Free DNase Set (Qiagen) and the cDNA templates were synthesized using ReverTra Ace qPCR RT Mix with genomic DNA (gDNA) Remover (TOYOBO) for RT-PCR Total RNA was extracted using the RNeasy Plant Mini Kit (Qiagen) and the RNase-Free DNase Set (Qiagen). The cDNA library was constructed using TrueSeq Stranded mRNA LT Sample Prep Kit (Illumina), and sequenced by NovaSeq 6000 (Illumina) with 101-base pair (bp) paired-end reads.

The paired-end reads were then mapped onto tomato reference genome (ITAG4.1) using Hisat2.

Hatching factor extraction

For the preparation of hatching assay samples, each hairy root culture solution was loaded onto a column placed one-tenth amount of Sepabeads SP207 resin pre-washed and equilibrated with three times resin volumes of methanol and water, respectively. The column was washed and eluted with three resin column volumes of water and methanol, respectively. The eluents were dried in vacuo and dissolved in water with the same ratio of original culture solution. For the hatching factor analysis using LC-MS/MS, remaining culture solutions were combined from three independent flask and loaded onto a column in 20 ml of SP207 resin. The column was washed with 20 and 60 ml of water and 20% (v/v) aqueous methanol, respectively, and eluted with 60 ml of methanol. The methanol eluents were dried in vacuo and re-dissolved in 100 μ l of methanol. The LC-MS/MS analytical condition was as described in “Chapter 2”.

Hatching assay

Hatching assay was conducted as described in “Chapter 1”.

Result

Effects of oxygenase inhibitors on HF biosynthesis

The solanoecelepin A and B are classified as triterpenoid, therefore I estimated their biosynthesis occur in similar mechanism of general triterpenoid synthesis. The first committed step of triterpenoid biosynthesis is the cyclization of 2,3-oxidosqualene,

resulting in the formation of the primary cyclized skeleton, and then vast array of the biosynthetic enzymes such as oxygenase like cytochrome P450 monooxygenase (CYP) and 2-oxoglutarate dependent dioxygenase (DOX), oxidoreductase, transferase, are involved to modify or rearrange the structure. In plant genome, CYP and DOX genes form large gene families, called as superfamily. CYPs are heme-thiolate membrane proteins and anchoring to the endoplasmic reticulum, while DOXs are no-heme iron containing proteins and localized in cytoplasm^{37,35}. Focused on the fact that SEB is a highly oxygenated triterpenoid with nine oxygens, several steps of oxygenation reaction are involved in its biosynthesis. I therefore conducted the inhibitor treatment using tomato hairy root culture system and evaluated the effect on HS activity. The treatment with each of oxygenase inhibitors, uniconazole P and prohexadione which inhibit CYPs and DOXs, respectively, was shown to decrease the hatching rate compared to that of mock treatment (Figure 3-7). The inhibition of each oxygenase enzymes resulted in the decrease in HS activity, suggesting that at least one of each enzyme is involved in the SEB biosynthesis.

Root specific occurrence of HF production

Most plant specialized metabolites are biosynthesized tissue-specifically, as well as the gene expression of their biosynthetic genes. To investigate in which tissue HFs are biosynthesized, I extracted hydroponically cultivated tomato tissues and evaluated their HS activity. The significant HS activity was observed in all tissues, with the most potent in roots (Figure 3-8A). Moreover, when comparing with roots and the corresponding amounts of root exudates, the root exudates showed 10-fold higher HS activity, suggesting that the HFs are specifically biosynthesized in roots and immediately

excreted into the culture solution or soil environment (Figure 3-8B).

Selection of candidate solanoeclepin biosynthetic gene.

Based on the above result, I selected the candidate genes involved in the HF biosynthesis in terms of the genes encoding CYP or DOX and specifically expressed in roots. The DOXs form one of the largest enzyme superfamilies in plant kingdom and associated with the oxygenation reactions of various specialized metabolites, including triterpenoids^{35,25,38}. I obtained the tomato genes encoding DOX and tissue specific RNA-seq data from Sol Genomics Network (<https://solgenomics.net/>) and 31 *DOX* genes were specifically expressed in roots (Table 3-2). Among them, there were seven genes classified into *DOXC20* subfamily, which included genes recently identified and characterized as the biosynthetic genes for SGAs³⁸. Next, I conducted phylogenetic analysis of plant *DOXC20* subfamily. Five of seven genes specifically expressed in roots formed a gene cluster, and some *Fabaceae* genes orthologous to *Solyc06g067870* were confirmed (Figure 3-9). *Fabaceae* plants are damaged by soybean cyst nematode in similar manner of *Solanaceae* plants, and secret the hatching factors, glycinoclepin A, B, and C. Solanoeclepins and glycinoclepins are similar in structure and bioactivity, and thought to share similar biosynthetic pathways. I therefore selected *Solyc06g067870* as candidate gene and named as *SIDOX70*.

Generation of SIDOX70-disrupted hairy roots

To confirm whether *SIDOX70* is involved in HF biosynthesis, I generated the *SIDOX70*-disrupted hairy roots (*SIDOX70*-ko) and evaluated the HS activity of transgenic hairy roots. The CRISPR/Cas9 genome editing system was used for candidate gene disruption

and three independent guide RNAs were designed (Figure 3-2A). The transgenic hairy roots which confirmed any mutations (Figure 3-2B), were cultivated and subjected to the hatching assay. The result showed that the HS activity of *SIDOX70*-ko were reduced to less than one fifth of that of vector control hairy roots (Figure 3-10). I also conducted the LC-MS/MS analysis and the SEB was detected in the culture solution of vector control hairy roots, but not detected in that of *SIDOX70*-ko (Figure 3-11). I therefore identified *SIDOX70* as a SEB biosynthetic gene.

Selection of neighbor genes of SIDOX70 in phylogenetic tree as candidate biosynthetic genes

In the genome region of *SIDOX70* gene, six *DOX* genes are located in tandem and formed gene cluster (Figure 3-12). The biosynthetic genes of plant specialized metabolites are frequently located in neighbor in each other and form gene cluster³⁹. Thus, I next focused on *Solyc06g067860* which is located to next to *SIDOX70* in genome and named as *SIDOX60*. *Solyc12g042980*, which was located near *SIDOX70* and *SIDOX60* in the phylogenetic tree, was also selected as candidate biosynthetic gene and named as *SIDOX80*. The culture solution of *SIDOX60*- and *SIDOX80*-disrupted hairy roots (*SIDOX60*-ko and *SIDOX80*-ko) generated by the same way as *SIDOX70*-ko, exhibited the reduced HS activity and SEB disappearance (Figure 3-10, 3-11). The amino acid sequence identity between *SIDOX70* and *SIDOX60* are not high as 47%, suggesting that they are not functionally redundant enzymes but are independently involved in the SEB biosynthesis.

Gene expression analysis of SEB biosynthetic genes

In general, the biosynthetic genes of plant specialized metabolites are expressed in coordinated manner and some phytohormones regulate their gene expression such like jasmonate in regulation of the biosynthesis of defense compounds²¹. To investigate the gene expression response of SEB biosynthetic genes against phytohormones, I conducted the transcriptome analysis of phytohormone-treated tomato hairy roots. Compared with the fragment per kilobase exon per million mapped reads (FPKM) values of mock treatment, the value of each *DOX* gene was reduced in MeJA, IAA, and ABA treatment (Table 3-3). In contrast, no consistent effect was observed in the treatment with MeSA, GA3 and tZ (Table 3-3). These results suggest the hypothesis that solanoeclepin biosynthesis is down-regulated by MeJA, IAA, and ABA and not regulated by MeSA, GA3, and tZ.

Gene disruption of candidate CYP genes involved in HF biosynthesis

I further searched the candidate biosynthetic genes according to the above hypothesis, and selected Solyc05g011940 and Solyc05g011970 encoding SlCYP749A19 and SlCYP749A20, respectively (Table 3-4). Each gene disrupted hairy roots, *SlCYP749A19*-ko and *SlCYP749A20*-ko, exhibited the reduced HS activity and solanoeclepin B disappearance, indicating that they were also identified as solanoeclepin biosynthetic genes (Figure 3-13, 3-14).

Discussion

In this chapter, I investigate the HF biosynthesis and identified five oxygenase genes as HF biosynthetic gene. The knocking out of each biosynthetic gene in tomato hairy roots

exhibited the decrease of HS activity toward the PCN eggs as well as SEB was not detected. This means that the accumulated products in knocking out tomato hairy roots do not possess the sufficient HS activity. Therefore, each biosynthetic enzyme identified in this chapter are suggested to be located in upstream of HF biosynthetic pathway before the compound possess the HS activity. They suspected to be involved in the reaction step to build the essential chemical backbone or in the oxygenation reaction to be required for HS activity. However, the identification of accumulated products in knocking out hairy roots is challenging due to the trace amount. And the lack of the possible substrates of each biosynthetic enzyme makes it difficult to understand their detailed functions.

When the tomato hairy roots culture solution was subjected to Sepabeads SP207 purification, the collected HS activity was not sufficient to that of original culture solution, but recovered by combining all fractions, suggesting that the presence of the cofactor which enhance the HS activity (Figure 3-15). In the case of knocking out tomato hairy roots, the collected HS activity was dramatically decreased than that of vector control hairy roots. This inconsistent of the decreased degree due to the purification step was thought to be the presence of cofactor. Therefore, it was suggested that the HS activity of knocking out hairy roots was almost lost. The subsequent liquid phase separation resulted in the separation of the HS activity, and the HS activity of aqueous fraction also lost by gene disruption (Figure 3-16). Since the SEB was mainly extracted with the ethyl acetate, the HS activity exhibiting in the remaining aqueous phase was expected to be unidentified HFs, as is the same case in potato hydroponic culture solution in “Chapter 2”. A single gene disruption resulted in the loss of all HS activity, suggesting that the HFs in tomato including the unidentified compounds are the

biosynthetically related to the SEB.

The orthologous genes of *SIDOX70* are present in *Fabaceae* plants, whereas no orthologous gene of *SIDOX60*, *SIDOX80*, *SICYP749A19*, and *SICYP749A20* was confirmed. *Fabaceae* plants produce glycinoclepins which is thought to be share the partial biosynthetic pathway with solanoclepins. Therefore, the orthologous genes of *SIDOX70* in *Fabaceae* plants may be involved in the glycinoclepin biosynthesis, and the other four genes specifically function in solanoclepin biosynthesis. However, further studies are needed. To the best of my knowledge, the involvement of *CYP749* family gene in the biosynthesis of plant specialized metabolites has been reported so far. Therefore, the detailed functional characterization of *SICYP749A19* and *SICYP749A20* is also expected in terms of the research field of CYP diversification.

In conclusion, I identified the five biosynthetic genes involved in the solanoclepin biosynthesis, which are the first gene discovery in the world.

Concluding discussion

Potato cyst nematodes (PCNs) are one of the most harmful pests and cause serious damage on crop production. Due to the characteristic life cycle of PCN, especially in the hatching process, it is quite difficult to manage the damages by PCNs and to establish efficient counter measures. The hatching factors (HFs) are thought to have potential usage to develop the efficient counter measures. However, little is understood about the biosynthesis, excretion mechanism, and the significance in plant themselves to date. In this study, I designed to clarify the main character of HFs in host plant root exudates and to investigate the HF biosynthesis.

In “Chapter 1”, I investigate the contribution of steroidal glycoalkaloids (SGAs) on hatching stimulation (HS) activity in host plant hairy roots and its structure-activity relationship. SGAs significantly showed the HS activity toward the PCN eggs, but were estimated to affect little on the HS activity in the hairy roots culture solution of potato and tomato. The structural requirements of the HS activity of SGAs are dependent on the sugar moieties attached at the C3-hydroxyl group and the alkaloid property of their aglycones. The stereochemistry in the EF rings of their aglycone also affected the strength of the HS activity. On the other hands, previously identified HF with high HS activity, solanoelepin A (SEA), is not have such chemical properties, suggesting that the reception mechanism in PCN eggs is different.

In “Chapter 2”, I searched for and successfully identified a novel HF, solanoelepin B (SEB), from bulk potato hydroponic culture solution and estimated to be SEB as one of major HFs. The structure of SEB was determined as the structure almost identical to that of SEA with the substitution at C-2 ketone group to hydroxy group. I also confirmed the fact that tomato hairy roots produce the SEB but not SEA.

These results allow me to investigate the biosynthesis in tomato hairy roots using analytical method to detect SEB.

In “Chapter 3” I used the tomato hairy roots culture system and identified five biosynthetic genes encoding oxygenase. The gene disruption using CRISPR/Cas9 system in tomato hairy roots resulted in the decrease of HS activity and loss of SEB peak in LC-MS/MS analysis. Furthermore, I revealed that there are unidentified HFs in tomato hairy roots but all HFs are biosynthetically related to SEB, since a single biosynthetic gene disruption caused the loss of HS activity evaluated by hatching assay after partial purification.

PCNs are thought to be evolved to synchronize their life cycle to host plants so that they are able to efficiently propagate and reproduce. On the other hands, they never hatch in absent of HFs around them. The biosynthetic genes discovered in this study could be good marker genes for the breeding the HF-less crop or for generate HF-deficient crop using genome editing system.

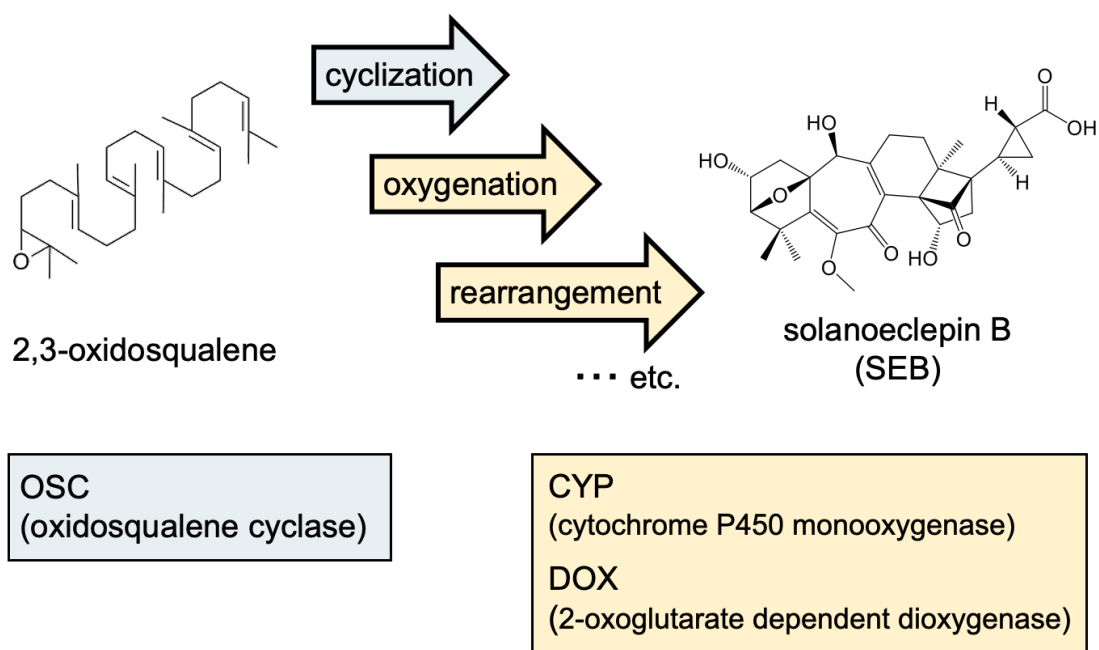


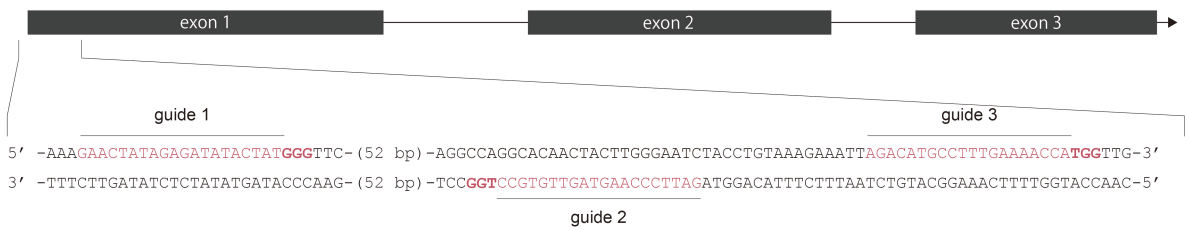
Figure 3-1. Putative biosynthesis of HFs.



Figure 3-2. The design of CPISPR/Cas9 construct for gene disruption of *SIDOX70*. (A) The sites of three target sequences. (B) The genotyping of sequences surrounding of the target sites in *SIDOX70*-ko hairy roots.

A

SIDOX60_Solyc06g067860



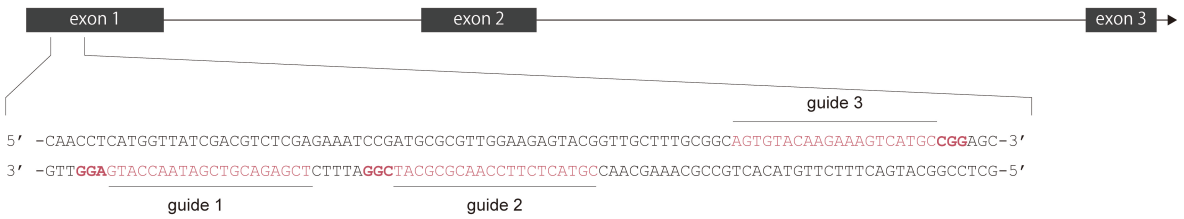
B



Figure 3-3. The design of CPISPR/Cas9 construct for gene disruption of *SIDOX60*
 (A) The sites of three target sequences. (B) The genotyping of sequences surrounding of the target sites in *SIDOX60*-ko hairy roots.

A

SIDOX80_Solyc12g042980



B

guide 1 guide 2 guide 3

WT: 5' -CAACCTCATGGTTATCGACGTCTCGASAAATCCGATGCGCGTTGGAAGAGTACGGTTGCTTTGCGGCAGTGTACAAGAAAGTCATGCCGGAGC-3'

#30: 5' -CAACCTCATG-----TGCCGGAGC-3'

Figure 3-4. The design of CPISPR/Cas9 construct for gene disruption of *SIDOX80*
 (A) The sites of three target sequences. (B) The genotyping of sequences surrounding of the target sites in *SIDOX80*-ko hairy roots.



Figure 3-5. The design of CPISPR/Cas9 construct for gene disruption of *SICYP749A19*
 (A) The sites of three target sequences. (B) The genotyping of sequences surrounding of the target sites in *SICYP749A19*-ko hairy roots.

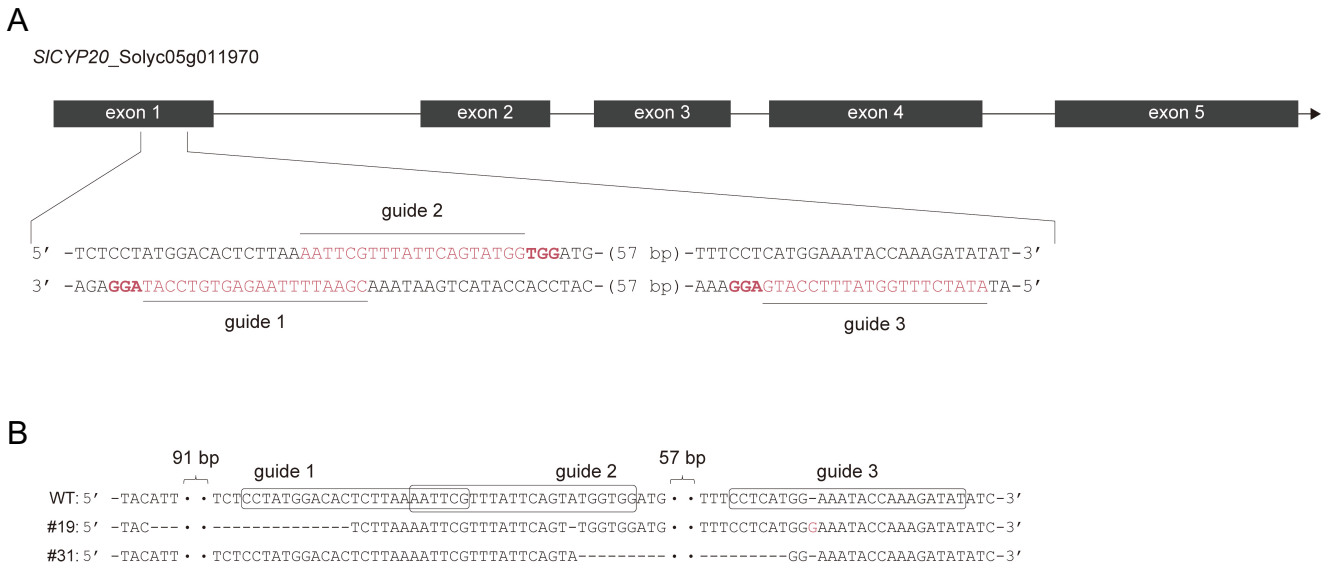


Figure 3-6. The design of CPISPR/Cas9 construct for gene disruption of *SICYP749A20*
 (A) The sites of three target sequences. (B) The genotyping of sequences surrounding of the target sites in *SICYP749A20*-ko hairy roots.

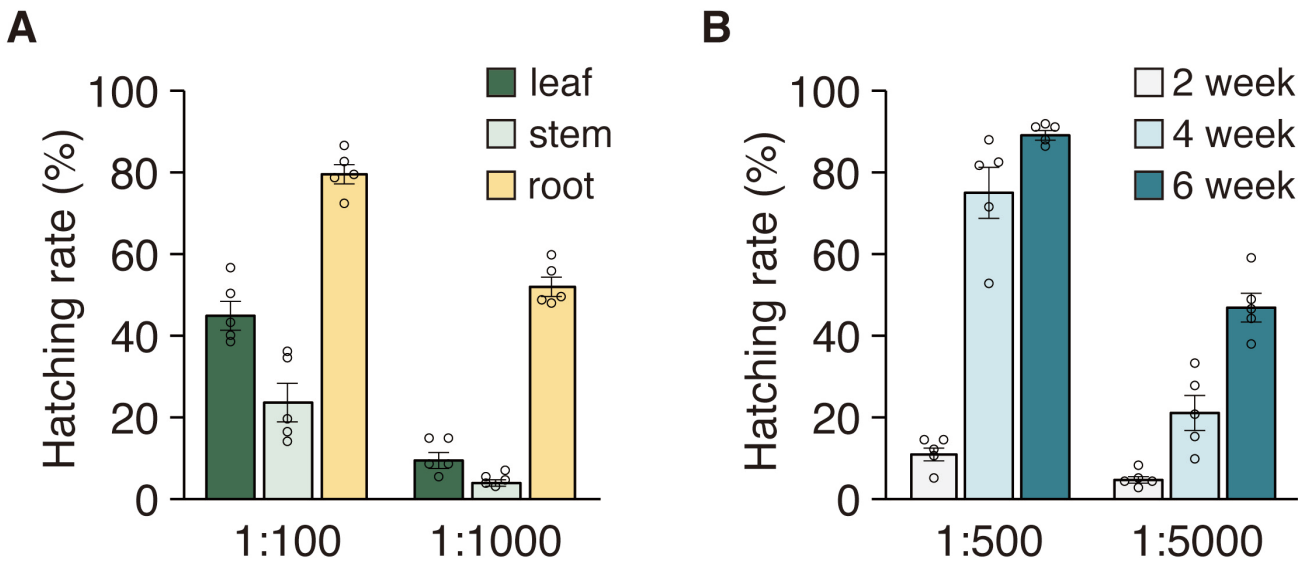


Figure 3-7. Hatching stimulation activity of plant tissue extracts or root exudates.

Hatching assay was conducted with eggs. The sample solutions were prepared by dissolving the extracts from 100 mg fresh weight of tomato tissue (A) or exudates corresponding to 100 mg fresh weight of 6-week-old tomato root (B) in 1 ml. For each sample solution, hatching assay was conducted in duplicates and two series of dilution were tested. The values are presented by mean \pm SE of five biological replicates.

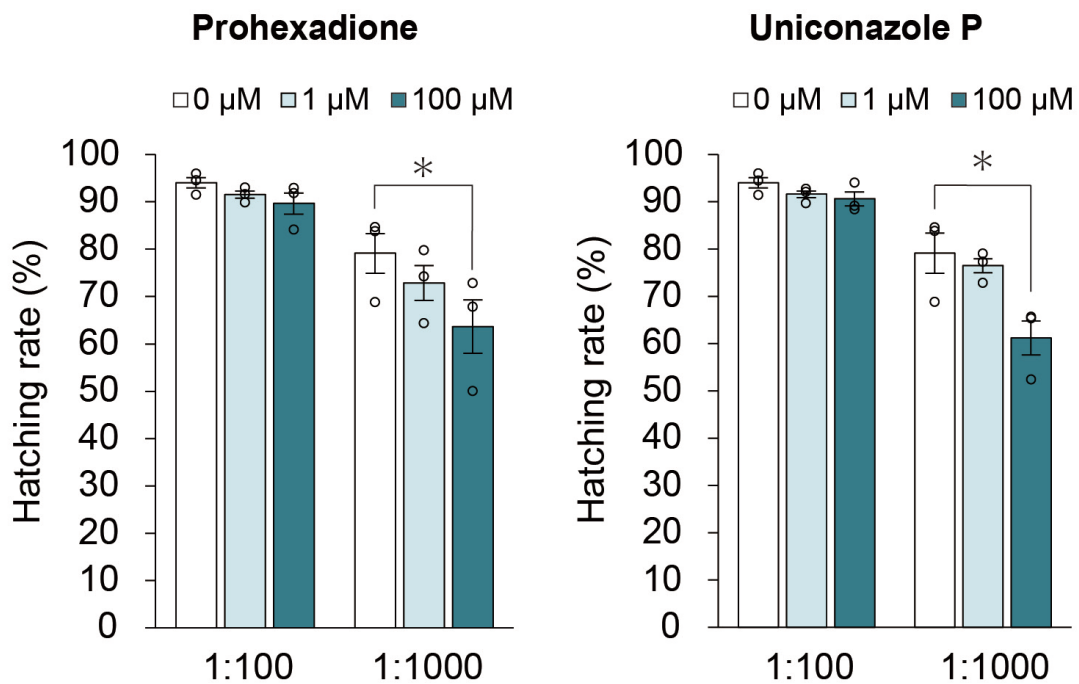


Figure 3-8. Effect of inhibitor treatment on hatching stimulation activity of hairy roots culture solution.

The hairy roots were treated with uniconazole P or prohexadione for three days. Hatching assay was conducted with Gr eggs. The values are presented by mean \pm SE of three biological replicates. For each sample solution, hatching assay was conducted in duplicates and two series of dilution (1:100 and 1:1000) were tested.

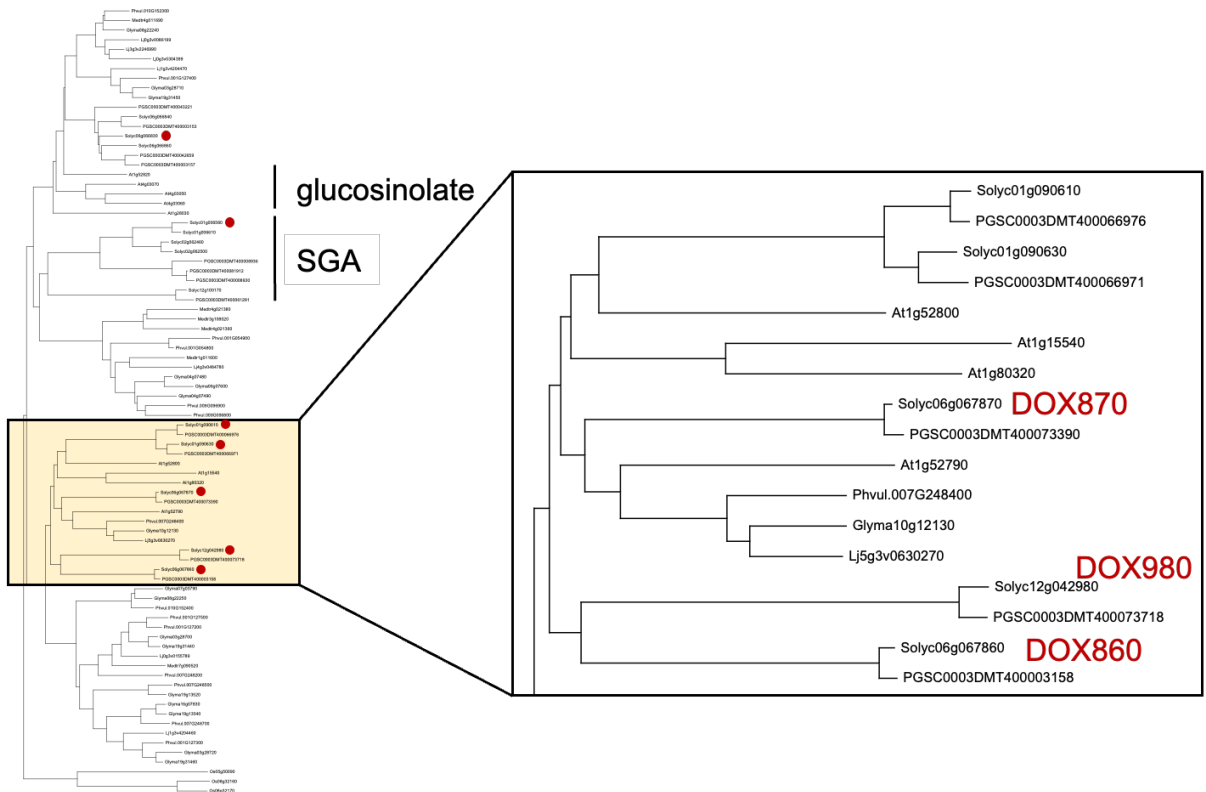


Figure 3-9. Phylogenetic tree of *DOXC20* subfamily genes.

The *DOXC20* family genes were obtained from *Solanum lycopersicum* (Solyc_), *S. tuberosum* (PGSC_), *Glycine max* (Glyma_), *Phaseolus vulgaris* (Phvul_), *Lotus japonicus* (Lj_), *Medicago truncatula* (Medtr_), *Arabidopsis thaliana* (At_). *Oryza sativa* *DOXC20* genes were used for out group.

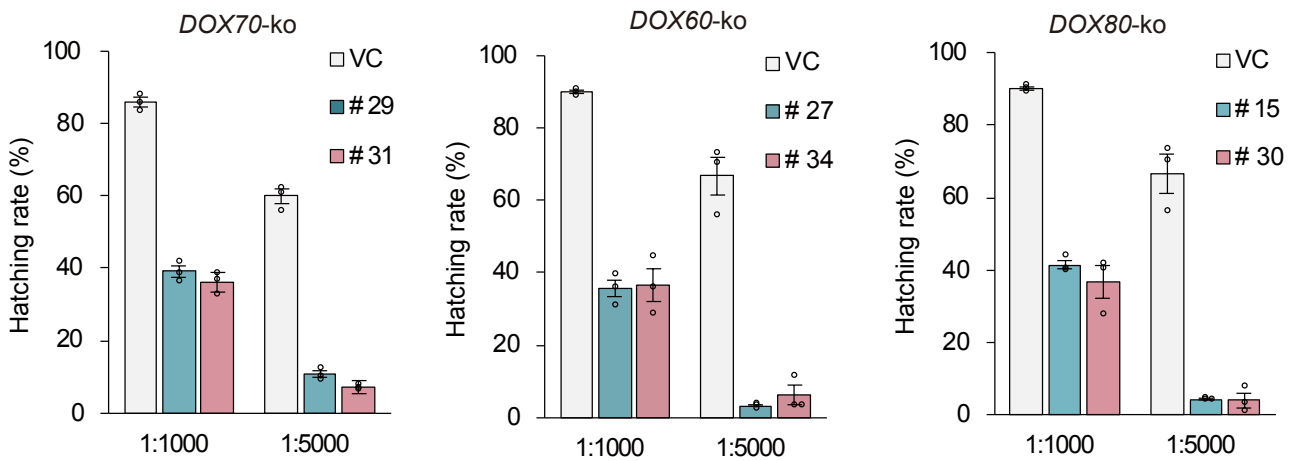


Figure 3-10. Decrease of HS activity by gene disruption of candidate *DOX* genes. Hatching assay was conducted with eggs. The sample solutions were prepared as the same concentration to the original hairy roots culture solution. For each sample solution, hatching assay was conducted in duplicates and two series of dilution were tested. The values are presented by mean \pm SE of three biological replicates.

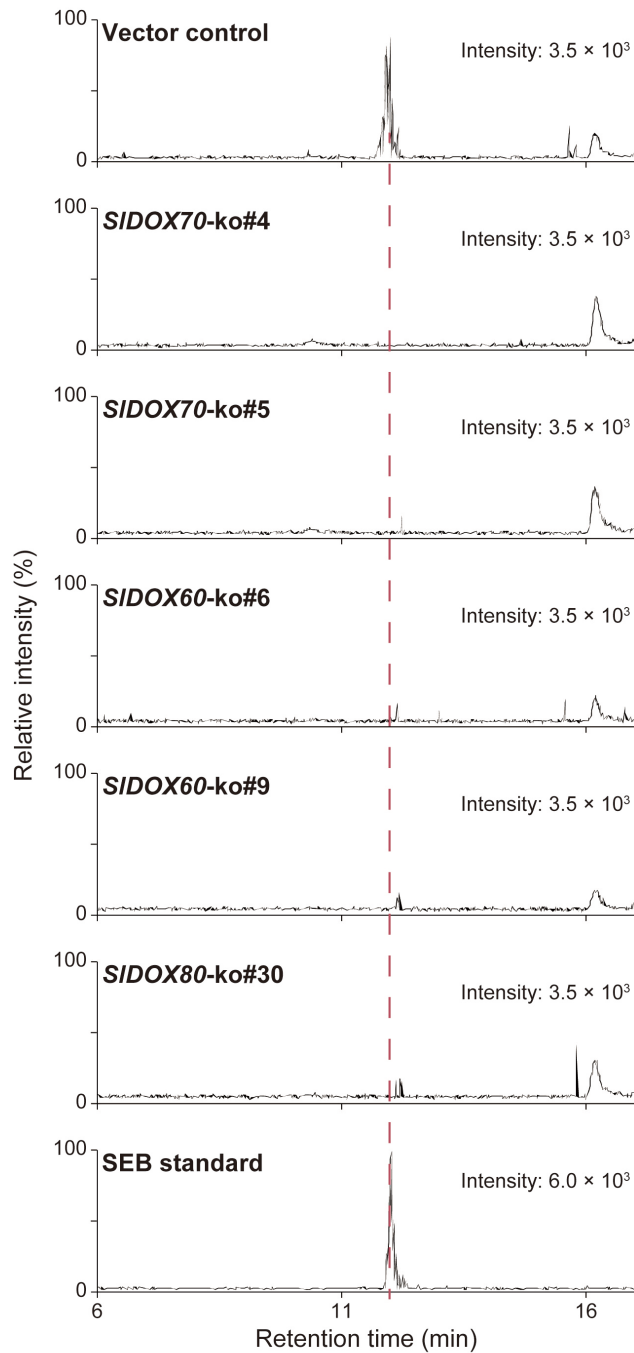


Figure 3-11. LC-MS/MS chromatograms of candidate *DOX* gene disrupting hairy roots. MRM chromatograms of each *DOX*-ko hairy roots culture solution. The MRM transition was selected as m/z 501 > 429 to detect SEB.



Figure 3-12. The *DOXC20* gene cluster on chromosome 6.

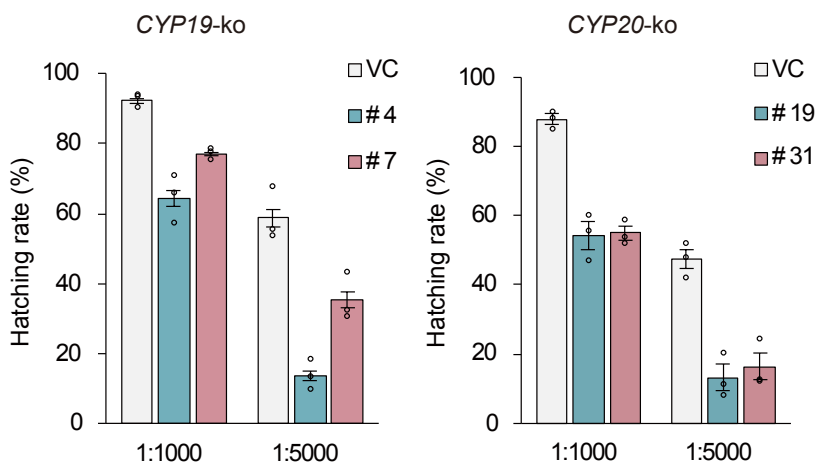


Figure 3-13. Decrease of HS activity by gene disruption of candidate *CYP* genes. Hatching assay was conducted with eggs. The sample solutions were prepared as the same concentration to the original hairy roots culture solution. For each sample solution, hatching assay was conducted in duplicates and two series of dilution were tested. The values are presented by mean \pm SE of three biological replicates.

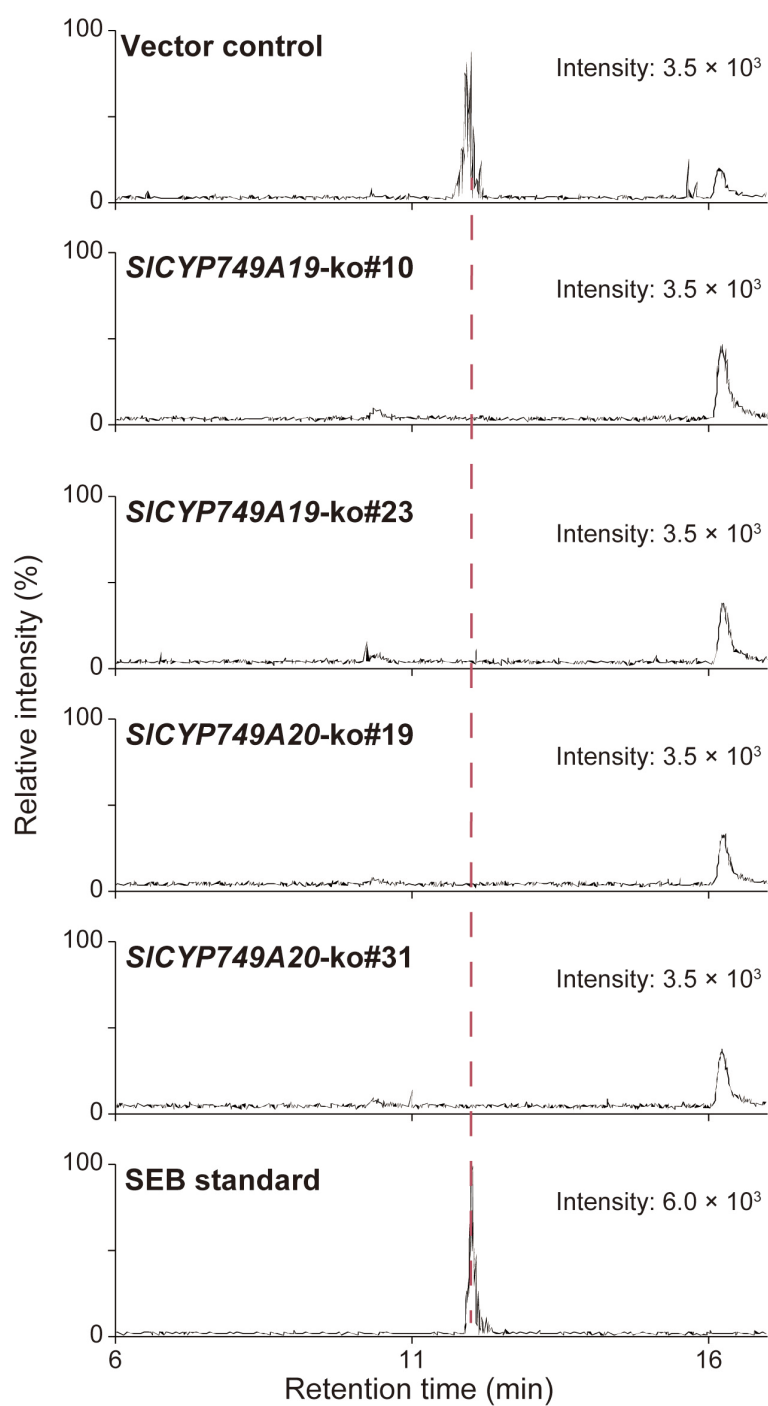


Figure 3-14. LC-MS/MS chromatograms of candidate *CYP* gene disrupting hairy roots. MRM chromatograms of each *CYP*-ko hairy roots culture solution. The MRM transition was selected as m/z 501 > 429 to detect SEB.

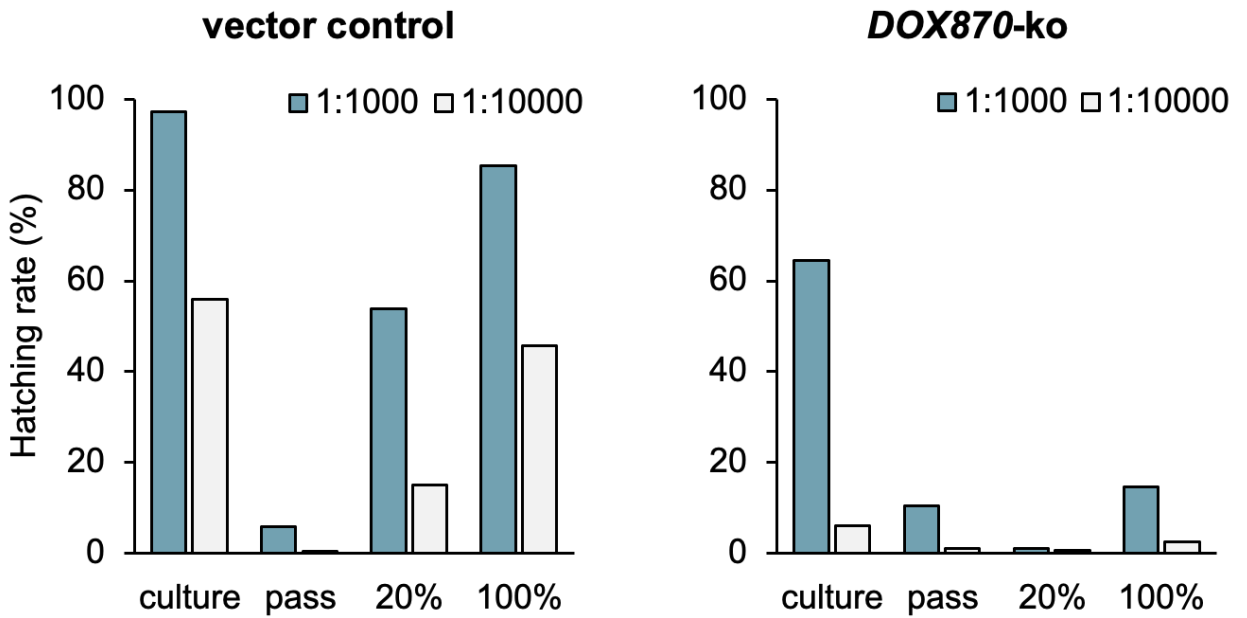


Figure 3-15. The behavior of HS activity by partial purification by Sepabeads SP207 resin Hatching assay was conducted with eggs. The sample solutions were prepared as the same concentration to the original hairy roots culture solution. For each sample solution, hatching assay was conducted in duplicates and two series of dilution were tested. The values are presented by mean \pm SE of three biological replicates

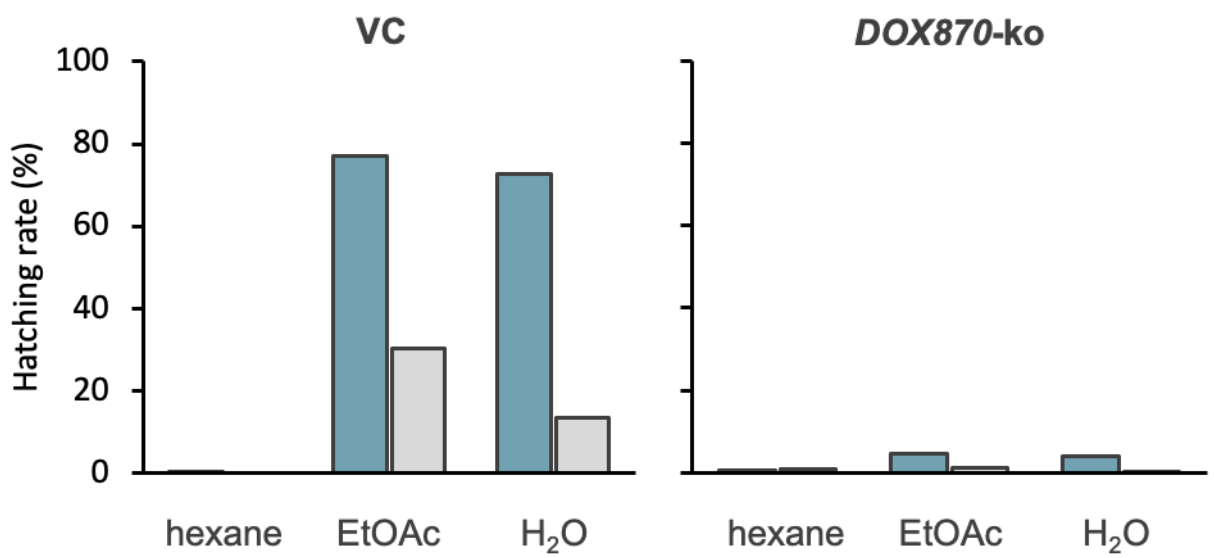


Figure 3-16. The behavior of HS activity by liquid phase extraction.

Table 3-1. Primer sequences used in this chapter.

Primer No.	Usage	Primer sequence (5' → 3')
Primer-1	For construction of CRISPR/Cas9 vector of <i>SIDOX70</i>	TTGGGTCTCGTGCAGTTGGACCATGAATTTGTACCGTTTTAGAGCTAGAAATAGCA
Primer-2		TTGGGTCTCGATAAACCATAACAAGTTTTAGAGCTAGAAATAGCA
Primer-3		TTGGGTCTCCTTATGTTGGCCACTGCACCAGCCGGGAATCGAA
Primer-4		TTGGGTCTCCAAACTTGTATGGTTATGTTGGCCACTGCACCAGCCGGGAATCGAA
Primer-5	For construction of CRISPR/Cas9 vector of <i>SIDOX60</i>	TTGGGTCTCGTGCAGAACTATAGAGATATACTATGTTTTAGAGCTAGAAATAGCA
Primer-6		TTGGGTCTCGAGTAGTTGTGCCGTTTTAGAGCTAGAAATAGCA
Primer-7		TTGGGTCTCCTACTTGGGAATCTGCACCAGCCGGGAATCGAA
Primer-8		TTGGGTCTCCAAACTGGTTTTCAAAGGCATGTCTCTGCACCAGCCGGGAATCGAA
Primer-9	For construction of CRISPR/Cas9 vector of <i>SIDOX80</i>	TTGGGTCTCGTGCAGTCGAGACGTCGATAACCATGGTTTTAGAGCTAGAAATAGCA
Primer-10		TTGGGTCTCGTCCAACGCGCATGTTTTAGAGCTAGAAATAGCA
Primer-11		TTGGGTCTCCTGGAAGAGTACGCTGCACCAGCCGGGAATCGAA
Primer-12		TTGGGTCTCCAAACGCATGACTTCTTGTACACTCTGCACCAGCCGGGAATCGAA
Primer-13	For construction of CRISPR/Cas9 vector of <i>SICYP749A19</i>	TTGGGTCTCGTGCAGCAAGAAGCTTTTCGGAGACGGTTTTAGAGCTAGAAATAGCA
Primer-14		TTGGGTCTCGTGGGTAAAAATGGTTTTAGAGCTAGAAATAGCA
Primer-15		TTGGGTCTCCCCCATTTTTTCGCTGCACCAGCCGGGAATCGAA
Primer-16		TTGGGTCTCCAAACTGTTTTTCATGGAGTAAGCCTGCACCAGCCGGGAATCGAA
Primer-17	For construction of CRISPR/Cas9 vector of <i>SICYP749A20</i>	TTGGGTCTCGTGCAGTCGAGACGTCGATAACCATGGTTTTAGAGCTAGAAATAGCA
Primer-18		TTGGGTCTCGTCCAACGCGCATGTTTTAGAGCTAGAAATAGCA
Primer-19		TTGGGTCTCCTGGAAGAGTACGCTGCACCAGCCGGGAATCGAA
Primer-20		TTGGGTCTCCAAACGCATGACTTCTTGTACACTCTGCACCAGCCGGGAATCGAA
Primer-21	For genotyping of <i>SIDOX70</i> -ko (Fw)	AAGAAGCCTATATAAAACCAAGCAA
Primer-22	For genotyping of <i>SIDOX70</i> -ko (Rv)	TGGCCACATGAGGTTGGAAA
Primer-23	For genotyping of <i>SIDOX60</i> -ko (Fw)	GGGTTCTCTAACAGTTACCCACAA
Primer-24	For genotyping of <i>SIDOX60</i> -ko (Rv)	CCATTAGGCCACATGAAATGGT
Primer-25	For genotyping of <i>SIDOX80</i> -ko (Fw)	TGGCTTCCAAGTAGAACCAA
Primer-26	For genotyping of <i>SIDOX80</i> -ko (Rv)	ACCAGTATTTATGAACGTTGTCATT
Primer-27	For genotyping of <i>SICYP749A19</i> -ko (Fw)	CTCTACTGGCATGGACTGCAA
Primer-28	For genotyping of <i>SICYP749A19</i> -ko (Rv)	TTCCAACGTTTCGAGCATTGTCT
Primer-29	For genotyping of <i>SICYP749A20</i> -ko (Fw)	TCCCTACACATCATTATCAAAAGCC
Primer-30	For genotyping of <i>SICYP749A20</i> -ko (Rv)	TACCGTACATCCTTGTCCATGTG

Table 3-2. Candidate *DOX* list

Gene ID	DOX subfamily	Gene name	Bud	Flower	Leaf	Root	Fruits stage			
							1cm	2cm	3cm	Mature green
Solyc01g108860	DOXC21		0	0	0	1345	0	0	0	1
Solyc01g090610	DOXC20		0	0	0	648	0	0	0	0
Solyc06g066830	DOXC20		0	0	0	282	0	0	0	0
Solyc12g042980	DOXC20	DOX80	0	0	0	180	0	0	0	0
Solyc06g067860	DOXC20	DOX60	0	0	0	152	0	0	0	0
Solyc11g072200	DOXC41		0	0	0	139	0	0	0	0
Solyc06g067870	DOXC20	DOX70	0	0	2	128	0	0	0	0
Solyc01g090630	DOXC20		0	0	0	94	0	0	0	0
Solyc02g071470	DOXC52		0	0	2	87	0	1	1	8
Solyc09g089830	DOXC22		0	0	0	83	0	0	0	0
Solyc06g083910	DOXC38		1	0	0	75	0	0	0	0
Solyc02g070080	DOXC38		0	0	0	67	0	0	0	0
Solyc09g089680	DOXC31		1	3	1	43	0	0	0	2
Solyc11g010400	DOXC38		0	0	0	41	0	0	0	0
Solyc03g116260	DOXC22		0	1	1	38	0	0	0	0
Solyc01g067620	DOXC54		3	15	0	36	0	1	1	0
Solyc06g073580	DOXC38		2	0	0	26	0	0	0	0
Solyc06g069900	DOXC22		0	0	0	20	0	0	0	0
Solyc01g006580	DOXC20		0	0	0	19	0	0	0	0
Solyc09g089790	DOXC31		0	1	0	18	0	0	0	0
Solyc06g060070	DOXC53		5	1	0	17	0	0	0	0
Solyc03g120970	DOXC3		2	1	2	14	2	1	1	1
Solyc02g071440	DOXC52		4	2	0	12	0	1	0	0
Solyc02g071410	DOXC52		1	1	0	12	0	0	1	1
Solyc02g071490	DOXC52		2	1	0	11	1	2	2	2
Solyc09g089780	DOXC31		0	0	0	8	0	0	0	0
Solyc09g089810	DOXC31		0	0	0	7	0	0	0	0
Solyc07g045040	DOXC55		0	0	0	6	0	0	0	0
Solyc03g025490	DOXC17		0	0	0	5	0	0	0	0
Solyc09g089800	DOXC31		0	0	0	5	0	0	0	0
Solyc07g054870	DOXC37		0	0	1	5	0	0	0	0

Table 3-3. *DOX* gene expression profiles in response to phytohormones.

Gene ID	DOX subfamily	Gene name	Treatment						
			Mock	MeJA	MeSA	IAA	GA3	ABA	tZ
Solyc01g090610	DOXC20		127.21	46.82	149.11	6.38	94.77	33.44	50.14
Solyc02g070080	DOXC41		8.21	0.53	6.11	0.31	7.03	2.28	6.13
Solyc02g071470	DOXC52		30.28	14.85	37.18	9.14	21.03	4.17	11.77
Solyc06g066830	DOXC20		100.19	1.01	83.51	0.88	13.64	0.19	12.62
Solyc06g067860	DOXC20	DOX60	84.83	14.81	68.43	1.80	38.66	2.97	33.17
Solyc06g067870	DOXC20	DOX70	71.50	4.42	55.02	0.54	17.81	3.72	18.68
Solyc06g069900	DOXC22		10.76	4.66	11.82	1.32	3.99	0.49	4.22
Solyc09g066320	DOXC38		3.24	1.32	3.28	0.77	1.18	0.29	1.67
Solyc09g089760	DOXC31		9.50	3.42	10.20	2.74	4.40	2.96	1.22
Solyc09g089800	DOXC31		4.89	1.74	5.62	1.03	4.34	1.99	2.23
Solyc09g089830	DOXC22		77.18	24.04	76.78	5.27	49.66	10.22	29.30
Solyc11g007890	DOXC37		1.01	0.09	0.92	0.45	0.64	0.03	1.14
Solyc11g010400	DOXC41		14.53	6.69	23.27	1.93	26.24	3.09	11.58
Solyc11g045520	DOXC30		8.15	0.35	4.45	3.84	6.19	0.09	10.96
Solyc12g042980	DOXC20	DOX80	32.09	0.09	58.24	0.17	44.21	0.16	38.16

Table 3-4. CYP gene expression profiles in response to phytohormones.

Gene ID	CYP family	Treatment						
		Mock	MeJA	MeSA	IAA	GA3	ABA	tZ
Solyc01g009370	CYP98A55	78.36	17.04	45.87	18.06	79.92	27.69	98.09
Solyc01g080120	-	1.38	0.05	1.18	0.61	0.88	0.20	1.25
Solyc01g094120	CYP704A65	0.95	0.00	1.31	0.02	0.45	0.34	0.70
Solyc02g069600	CYP716C6	8.51	1.60	6.02	2.43	6.21	0.91	4.21
Solyc02g094860	CYP735A20	24.00	2.63	17.39	0.20	15.87	9.44	9.44
Solyc03g112040	CYP71AU32	5.15	0.25	4.85	0.46	1.76	0.06	2.05
Solyc03g114940	CYP78A75	2.20	0.64	1.86	0.71	3.09	0.71	6.27
Solyc04g080650	CYP722A1	0.77	0.05	1.07	0.29	0.50	0.05	0.49
Solyc05g011940	CYP749A19	9.93	0.68	10.63	0.26	5.43	0.85	3.26
Solyc05g011970	CYP749A20	38.42	5.07	53.94	7.84	28.81	11.25	13.53
Solyc06g065430	CYP716E26	9.05	3.44	8.95	1.15	3.65	1.66	4.77
Solyc06g084825	-	0.01	0.00	0.00	0.00	0.00	0.00	0.00
Solyc07g061980	CYP72A183	0.45	0.05	0.35	0.07	0.13	0.08	0.36
Solyc08g079285	-	0.10	0.00	0.05	0.02	0.01	0.03	0.00
Solyc09g008913	-	4.55	2.27	4.47	0.92	4.74	1.24	1.59
Solyc09g098620	CYP76G10	3.26	0.85	3.55	0.02	1.43	0.03	1.66
Solyc10g039210	CYP82M2	3.16	0.42	3.99	0.13	3.88	1.46	3.60
Solyc10g087035	-	0.35	0.05	0.24	0.16	0.29	0.06	0.07
Solyc10g150144	-	0.03	0.00	0.00	0.00	0.00	0.00	0.00
Solyc12g088970	CYP82C22	2.55	0.12	1.30	0.72	3.92	0.02	0.17

Acknowledgement 謝辞

本研究を進めるにあたり、終始懇切なるご指導とご鞭撻賜り、本論文をまとめるに際して、親身なご助言をいただきました、水谷正治 准教授 (神戸大学大学院農学研究科) に心より感謝を申し上げます。

本研究および本論文作成の過程における議論・検討にあたって多大なるご教示ならびにご激励を賜りました杉本幸裕 教授 (神戸大学大学院農学研究科), ならびに本論文の審査において有益な議論と情報交換をしていただきました宇野知秀 教授 (神戸大学大学院農学研究科) に深く御礼申し上げます。また、本研究について貴重なご助言をいただきました山内靖雄 准教授 (神戸大学大学院農学研究科) に深謝申し上げます。

これまでの研究において、バイオアッセイ試験を行っていただき、様々なご助言をいただきました串田敦彦 博士 (農研機構・北海道農業研究センター), 合成品の solanoeclepin A のご恵与いただきました谷野圭持 教授 (北海道大学大学院総合化学院), NMR 構造解析等を行っていただきました渡辺文太 助教授 (京都大学化学研究所), ゲノム編集ベクターのご恵与いただきました刑部敬史 教授 (徳島大学生物資源産業学部), 刑部祐里子 教授 (東京工業大学生命理工学院) に深く御礼申し上げます。

植物機能化学研究室のみなさまには、大変お世話になりました。特に、共に研究を進めてきました秋山遼太 博士, 増田裕貴 さん, 岡村勇哉 さん, 小川千景 さんには多くの示唆と刺激をいただき、感謝の念に堪えません。お一人お一人のお名前を挙げることはできませんが、それぞれのお立場から研究から私生活においてまで様々な形でお力添えをいただきました。本当にありがとうございました。

Reference

1. Weng, J. K., Lynch, J. H., Matos, J. O. & Dudareva, N. Adaptive mechanisms of plant specialized metabolism connecting chemistry to function. *Nature Chemical Biology* vol. 17 1037–1045 (2021).
2. Sugiyama, A. The soybean rhizosphere: Metabolites, microbes, and beyond—A review. *J. Adv. Res.* **19**, 67–73 (2019).
3. van Dam, N. M. & Bouwmeester, H. J. Metabolomics in the Rhizosphere: Tapping into Belowground Chemical Communication. *Trends Plant Sci.* **21**, 256–265 (2016).
4. Dong, W. & Song, Y. The Significance of Flavonoids in the Process of Biological Nitrogen Fixation. *Int. J. Mol. Sci.* **21**, 5926 (2020).
5. Jones, J. T. *et al.* Top 10 plant-parasitic nematodes in molecular plant pathology. *Mol. Plant Pathol.* **14**, 946–961 (2013).
6. Nicol, J. M. *et al.* Current Nematode Threats to World Agriculture. in *Genomics and Molecular Genetics of Plant-Nematode Interactions* 21–43 (2011).
doi:10.1007/978-94-007-0434-3_2.
7. Williamson, V. M. & Gleason, C. A. Plant-nematode interactions. *Current Opinion in Plant Biology* vol. 6 327–333 (2003).
8. Sullivan, M. J., Inserra, R. N., Franco, J., Moreno-Leheudé, I. & Greco, N. Potato cyst nematodes: Plant host status and their regulatory impact. *Nematropica* vol. 37 193–201 (2007).
9. Masamune T, Anetai M, Takasugi M, Katsui N. Isolation of a natural hatching stimulus, glycinoeclepin A, for the soybean cyst nematode. *Nature* **297**, 495–496 (1982).

10. Fukuzawa, A., Matsue, H., Ikura, M. & Masamune, T. Glycinoeclepins B and C, nortriterpenes related to glycinoeclepin a. *Tetrahedron Lett.* **26**, 5539–5542 (1985).
11. Mulder, J. G., Diepenhorst, P., Plieger, P. & Bruggemann-Rotgans, I. E. M. Hatching agent for the potato cyst nematode. *Chem. Abstr.* **118**, 185844z (1992).
12. Schenk, H. *et al.* Elucidation of the Structure of Solanoeclepin A, a Natural Hatching Factor of Potato and Tomato Cyst Nematodes, by Single-crystal X-ray Diffraction. *Croat. Chem. Acta* **72**, 593–606 (1999).
13. Tanino, K. *et al.* Total synthesis of solanoeclepin A. *Nat. Chem.* **3**, 484–488 (2011).
14. Corey, E. J. & Houpis, I. N. Total Synthesis of Glycinoeclepin A. *J. Am. Chem. Soc.* **112**, 8997–8998 (1990).
15. Mori, K. & Watanabe, H. Recent results in the synthesis of semiochemicals: synthesis of glycinoeclepin A. *Pure Appl. Chem.* **61**, 543–546 (1989).
16. Murai, A., Tanimoto, N., Sakamoto, N. & Masamune, T. Total Synthesis of Glycinoeclepin A. *J. Am. Chem. Soc.* **110**, 1985–1986 (1988).
17. Shiina, Y., Tomata, Y., Miyashita, M. & Tanino, K. Asymmetric Total Synthesis of Glycinoeclepin A: Generation of a Novel Bridgehead Anion Species. *Chem. Lett.* **39**, 835–837 (2010).
18. Watanabe, H. & Mori, K. Triterpenoid total synthesis. Part 2. Synthesis of glycinoeclepin A, a potent hatching stimulus for the soybean cyst nematode. *J. Chem. Soc. Perkin Trans. 1* 2919 (1991) doi:10.1039/p19910002919.
19. Byrne, J. T., Maher, N. J. & Jones, A. P. W. Comparative Responses of *Globodera rostochiensis* and *G. pallida* to Hatching Chemicals. *J. Nematol.* **33**,

- 195–202 (2001).
20. Devine, K. J., Byrne, J., Maher, N. & Jones, P. W. Resolution of natural hatching factors for golden potato cyst nematode, *Globodera rostochiensis*. *Ann. Appl. Biol.* **129**, 323–334 (1996).
 21. Thagun, C. *et al.* Jasmonate-Responsive ERF Transcription Factors Regulate Steroidal Glycoalkaloid Biosynthesis in Tomato. *Plant Cell Physiol.* **57**, 961–975 (2016).
 22. Lee, H. J. *et al.* Identification of a 3 β -hydroxysteroid dehydrogenase/ 3-ketosteroid reductase involved in α -tomatine biosynthesis in tomato. *Plant Cell Physiol.* **60**, 1304–1315 (2019).
 23. Ashikawa, I., Fukuzawa, A., Murai, A., Kamada, H. & Koshi, M. Production of potato cyst nematode hatching stimulus by hairy root cultures of tomato. *Agric. Biol. Chem.* **55**, 2025–2029 (1991).
 24. Nakayasu, M. *et al.* Generation of α -solanine-free hairy roots of potato by CRISPR/Cas9 mediated genome editing of the St16DOX gene. *Plant Physiol. Biochem.* **131**, 70–77 (2018).
 25. Nakayasu, M. *et al.* A dioxygenase catalyzes steroid 16 α -hydroxylation in steroidal glycoalkaloid biosynthesis. *Plant Physiol.* **175**, 120–133 (2017).
 26. Akiyama, R. *et al.* Characterization of steroid 5 α -reductase involved in α -tomatine biosynthesis in tomatoes. *Plant Biotechnol.* **36**, 253–263 (2019).
 27. Sawai, S. *et al.* Sterol Side Chain Reductase 2 Is a Key Enzyme in the Biosynthesis of Cholesterol , the Common Precursor of Toxic Steroidal Glycoalkaloids in Potato. **26**, 3763–3774 (2014).
 28. Yasumoto, S. *et al.* Efficient genome engineering using platinum talein potato.

- Plant Biotechnol.* **36**, 167–173 (2019).
29. Umemoto, N. *et al.* Two cytochrome P450 monooxygenases catalyze early hydroxylation steps in the potato steroid glycoalkaloid biosynthetic pathway. *Plant Physiol.* **171**, 2458–2467 (2016).
 30. Sugiyama, A. & Yazaki, K. Flavonoids in plant rhizospheres: Secretion, fate and their effects on biological communication. *Plant Biotechnology* vol. 31 431–443 (2014).
 31. van Dam, N. M. & Bouwmeester, H. J. Metabolomics in the Rhizosphere: Tapping into Belowground Chemical Communication. *Trends in Plant Science* vol. 21 256–265 (2016).
 32. Mosimann, H., Vogel, P., Pinkerton, A. A. & Kirschbaum, K. Highly Stereoselective Synthesis of Perhydro-8a-(hydroxymethyl)phenanthrene-1,2,4,5,7,8-hexol and Derivatives. *J. Org. Chem.* **62**, 3002–3007 (1997).
 33. Benningshof, J. C. J. *et al.* Studies towards the total synthesis of solanoecelepin A: Synthesis of the 7-oxabicyclo[2.2.1]heptane moiety and attempted seven-membered ring formation. *J. Chem. Soc. Perkin 1* **14**, 1693–1700 (2002).
 34. Guerrieri, A. *et al.* UPLC-MS/MS analysis and biological activity of the potato cyst nematode hatching stimulant, solanoecelepin A, in the root exudate of *Solanum* spp. *Planta* **254**, 112 (2021).
 35. Kawai, Y., Ono, E., Mizutani, M. Evolution and diversity of the 2-oxoglutarate-dependent dioxygenase superfamily in plants. *Plant J.* **78**, 328–343 (2014).
 36. Xiao, A. *et al.* CasOT: A genome-wide Cas9/gRNA off-target searching tool. *Bioinformatics* **30**, 1180–1182 (2014).
 37. Mizutani M, Ohta D. Diversification of P450 Genes During Land Plant

- Evolution. *Annu. Rev. Plant Biol* **61**, 291–315 (2010).
38. Akiyama, R. *et al.* The biosynthetic pathway of potato solanidanes diverged from that of spirosolanes due to evolution of a dioxygenase. *Nat. Commun.* **12**, (2021).
 39. Liu, Z. *et al.* Formation and diversification of a paradigm biosynthetic gene cluster in plants. *Nat. Commun.* **11**, 5354 (2020).